Progress of Theoretical Physics, Vol. 119, No. 1, January 2008

Microscopic Derivation of Collective Hamiltonian by Means of the Adiabatic Self-Consistent Collective Coordinate Method

—— *Shape Mixing in Low-Lying States of* ^{68}*Se and* ^{72}*Kr* ——

Nobuo HINOHARA,[1] Takashi NAKATSUKASA,[2] Masayuki MATSUO[3] and Kenichi MATSUYANAGI[1]

[1]*Department of Physics, Graduate School of Science, Kyoto University, Kyoto 606-8502, Japan*
[2]*Theoretical Nuclear Physics Laboratory, RIKEN Nishina Center, Wako 351-0198, Japan*
[3]*Department of Physics, Faculty of Science, Niigata University, Niigata 950-2181, Japan*

(Received November 2, 2007)

The microscopic dynamics of oblate-prolate shape coexistence/mixing phenomena in ^{68}Se and ^{72}Kr are studied by means of the adiabatic self-consistent collective coordinate (ASCC) method in conjunction with the pairing-plus-quadrupole (P+Q) Hamiltonian, including the quadrupole pairing interaction. A quantum collective Hamiltonian is constructed, and excitation spectra, spectroscopic quadrupole moments and quadrupole transition properties are evaluated. The effect of the time-odd pair field on the collective mass (inertia function) of the large-amplitude vibration and the rotational moments of inertia about three principal axes is evaluated. It is found that the basic properties of the shape coexistence/mixing are qualitatively reproduced. The results of the calculation indicate that the oblate-prolate shape mixing decreases as the angular momentum increases.

§1. Introduction

Obtaining a microscopic understanding of nuclear collective dynamics is one of the goals of nuclear structure theory. The quasiparticle random phase approximation (QRPA), based on the Hartree-Fock-Bogoliubov (HFB) mean field, is a well-known theoretical approach to the collective dynamics, but it is applicable only to small-amplitude collective motion around the local minima of the potential energy surface.[1)–5)] Nuclei exhibit a variety of large-amplitude collective processes such as anharmonic vibrations, shape coexistence, and fission. Though the challenge to construct microscopic theories of large-amplitude collective motion has a long history,[6)–42)] some important problems remain unsolved.

The self-consistent collective coordinate (SCC) method[12),23)] is a microscopic theory of large-amplitude collective motion. This method, with the (η^*, η) expansion technique, enables us to extract the collective variables from the many-dimensional phase space associated with the time-dependent Hartree-Fock-Bogoliubov (TDHFB) state vectors, and to derive the collective Hamiltonian starting from a microscopic Hamiltonian. The SCC method has been successfully applied to various kinds of non-linear phenomena in nuclei, such as anharmonic γ-vibrations,[43)–46)] shape phase

transitions,[47)–50)] two-phonon states[51)] and collective rotations.[52)–54)] The (η^*, η) expansion is not necessarily convenient, however, for large-amplitude collective motion like shape coexistence/mixing phenomena, in which a microscopic description of the many-body tunneling effect between different local minima in the collective potential energy surface becomes the major task.

The adiabatic SCC (ASCC) method[55)] is an alternative way of solving the basic equations of the SCC method, assuming that the large-amplitude collective motion of interest is slow (adiabatic). Under this assumption, the basic equations of the SCC method are expanded up to second order with respect to the collective momentum, but the collective coordinate is treated non-perturbatively. Quite recently, we have given a rigorous formulation of the ASCC method in which the gauge invariance with respect to the particle number fluctuation degrees of freedom is taken into account.[56)]

As is well known, in contrast to the significant progress in the calculation of the collective potential energy, the present status of the microscopic theory is quite unsatisfactory with regard to the evaluation of the collective mass (inertia function) associated with the collective kinetic energy. Although the Inglis-Belyaev cranking mass is widely used, it violates self-consistency by ignoring the effect of the time-odd component of the moving mean field.[1)] The time-odd mean-field effect is taken into account in the collective mass derived with the QRPA, but its application is restricted to small-amplitude collective motion around equilibrium states. Concerning large-amplitude collective motion, though the effect of the time-odd component generated by the residual particle-hole interaction was investigated a few decades ago,[14)] the time-odd effect generated by the residual pairing interaction has not yet been studied. Quite recently, we showed, using the ASCC method in conjunction with the schematic model Hamiltonian,[58)–61)] that the time-odd pair field increases the collective mass.[57)] It remains to be seen, however, how it affects the shape coexistence dynamics discussed below.

Let us consider recent experimental data of interest. The shapes of nuclei along the $N = Z$ line change significantly as the numbers of protons and neutrons change.[62)–66)] The HFB calculation[67)] indicates that various shapes will appear along the $N = Z$ lines: a triaxial ground state for ^{64}Ge, oblate ground states for ^{68}Se and ^{72}Kr, strongly deformed prolate ground states for ^{76}Sr, ^{80}Zr and ^{84}Mo. Furthermore, oblate and prolate states may coexist in these nuclei, other than^{64}Ge. In ^{68}Se and ^{72}Kr, the ground and excited states corresponding to oblate and prolate shapes have been found experimentally.[63)–65)] From the viewpoint of collective dynamics based on the mean-field theory, it is expected that the oblate and prolate shapes are mixed by the many-body tunneling effect through the potential barrier lying between the two local minima in the potential energy landscape. The low-lying states in ^{68}Se and ^{72}Kr have been investigated using various theoretical approaches beyond the mean-field approximation: large-scale shell model calculations for ^{68}Se using the pfg-shells outside the ^{56}Ni core,[68)] shell model Monte Carlo calculations for ^{72}Kr employing the pf-sdg shells,[69)] configuration mixing calculations for $^{72-78}$Kr on the basis of the particle number and angular momentum projected generator coordinate method,[70)] and the EXCITED VAMPIR variational calculation for ^{68}Se and ^{72}Kr.[71)–73)] Quite

recently, Almehed and Walet[36)–39)] discussed collective paths connecting the oblate and prolate minima in ^{68}Se and $^{72-78}$Kr by means of an approach similar to the ASCC method.

The ASCC method was first tested[74)] in a schematic model[58)–61)] and then it was applied[75)] to oblate-prolate shape coexistence phenomena in ^{68}Se and ^{72}Kr with use of the pairing-plus-quadrupole (P+Q) Hamiltonian.[76)–79)] In both nuclei, the one-dimensional collective path connecting the two local minima of the potential is extracted. It was found that the collective path runs approximately along the valley of the potential energy surface lying in the triaxial deformed region. This indicates that the triaxial degree of freedom is essential for the description of large-amplitude shape mixing in ^{68}Se and ^{72}Kr. In Ref. 75), however, requantization of the collective Hamiltonian was not carried out, and excitation spectra, electromagnetic transition probabilities, and shape mixing probabilities in individual eigenstates were not evaluated.

This paper presents the result of the first application of the gauge invariant formulation[56)] of the ASCC method to nuclear structure phenomena. Thus, its major thrust is directed at examining the feasibility of the gauge-invariant ASCC method for describing the shape coexistence/mixing phenomena. Hereafter, we call this new version the "ASCC method", dropping the adjective "gauge-invariant" for simplicity. A more detailed investigation of experimental data and comparison with other approaches are planned for the future. We derive the quantum collective Hamiltonian that describes the coupled collective motion of the large-amplitude vibration responsible for the oblate-prolate shape mixing and the three-dimensional rotation of the triaxial shape. To evaluate the rotational moments of inertia, we extend the well-known QRPA equation for rotational motion, which yields the Thouless-Valatin moment of inertia,[80)] to non-equibrium states that are defined in the moving-frame associated with large-amplitude vibrational motion. To clarify the role of the time-odd pair field in shape mixing dynamics, we investigate, with use of the P+Q Hamiltonian including the quadrupole pairing interaction, its effects on the collective mass of large-amplitude vibration, the rotational moments of inertia, the energy spectra, transition probabilities, and shape mixing probabilities in individual eigenstates.

This paper is organized as follows. The basic equations of the ASCC method are summarized in §2. The quasiparticle representation of the microscopic Hamiltonian is given in §3. The procedure for solving the ASCC equations is presented in §4. The collective Schrödinger equation is derived in §5. Results of numerical calculations for energy spectra, spectroscopic quadrupole moments and quadrupole transition probabilities of low-lying states in ^{68}Se and ^{72}Kr are presented and discussed in §6. Concluding remarks are given in §7.

A preliminary version of this work was previously reported in Ref. 81).

§2. The ASCC method

2.1. *Basic equations of the ASCC method*

We first summarize the basic equations of the ASCC method. The TDHFB state $|\phi(t)\rangle$ is written in terms of the collective variables as

$$|\phi(t)\rangle = |\phi(q,p,\boldsymbol{\varphi},\boldsymbol{n})\rangle = e^{-i\sum_\tau \varphi^{(\tau)}\tilde{N}^{(\tau)}}\,|\phi(q,p,\boldsymbol{n})\rangle\,, \tag{2·1}$$

where q and p represent the one-dimensional collective coordinate and the collective momentum, respectively. The variables $\boldsymbol{\varphi} = (\varphi^{(n)}, \varphi^{(p)})$ and $\boldsymbol{n} = (n^{(n)}, n^{(p)})$ denote the gauge angles in particle number space and number fluctuations, respectively, which correspond to the canonical coordinates and momenta of the pairing rotation restoring the particle number conservation broken by the HFB approximation. The operator $\tilde{N}^{(\tau)} \equiv \hat{N}^{(\tau)} - N_0^{(\tau)}$ represents the particle number measured with respect to the reference value $N_0^{(\tau)}$, which is set to the number of the valence protons ($\tau = p$) and neutrons ($\tau = n$) in the model space.

The intrinsic state with respect to the pairing rotation is written $|\phi(q,p,\boldsymbol{n})\rangle = e^{i\hat{G}(q,p,\boldsymbol{n})}\,|\phi(q)\rangle$, where $|\phi(q)\rangle \equiv |\phi(q,p=0,\boldsymbol{n}=\boldsymbol{0})\rangle$. Assuming that large-amplitude collective motion is adiabatic, that is, the collective momentum p and the number fluctuation $\boldsymbol{n}$ are small, we expand the one-body operator $\hat{G}(q,p,\boldsymbol{n})$ with respect to p and $n^{(\tau)}$ and consider only the first order:

$$|\phi(q,p,\boldsymbol{n})\rangle = e^{ip\hat{Q}(q)+i\sum_\tau n^{(\tau)}\hat{\Theta}^{(\tau)}(q)}\,|\phi(q)\rangle\,. \tag{2·2}$$

Here, $\hat{Q}(q)$ is a time-even one-body operator, while $\hat{\Theta}^{(\tau)}(q)$ is a time-odd one-body operator. Using the quasiparticle creation and annihilation operators, $a^\dagger_\alpha(q)$ and $a_\alpha(q)$, defined with respect to a moving-frame HFB state $|\phi(q)\rangle$, which satisfy the condition $a_\alpha(q)\,|\phi(q)\rangle = 0$, they can be written as

$$\begin{aligned}\hat{Q}(q) &= \hat{Q}^A(q) + \hat{Q}^B(q) \\ &= \sum_{\alpha\beta}\left(Q^A_{\alpha\beta}(q)a^\dagger_\alpha(q)a^\dagger_\beta(q) + Q^{A*}_{\alpha\beta}(q)a_\beta(q)a_\alpha(q) + Q^B_{\alpha\beta}(q)a^\dagger_\alpha(q)a_\beta(q)\right), \qquad (2·3)\\ \hat{\Theta}^{(\tau)}(q) &= \sum_{\alpha\beta}\left(\Theta^{(\tau)A}_{\alpha\beta}(q)a^\dagger_\alpha(q)a^\dagger_\beta(q) + \Theta^{(\tau)A*}_{\alpha\beta}(q)a_\beta(q)a_\alpha(q)\right). \qquad (2·4)\end{aligned}$$

Note that the operator $\hat{Q}(q)$ contains the B-part (the third term in the r.h.s.), in addition to the A-part (the first and second terms) in order to satisfy the gauge-invariance of the ASCC equations.[56] In the following, we omit the index q in the quasiparticle operators for simplicity.

The basic equations of the SCC method consist of the canonical variable conditions, the moving-frame HFB equation, and the moving-frame QRPA equations. Below we summarize the lowest-order expressions of these equations with respect to expansion in p and $\boldsymbol{n}$. (See Ref. 56) for their derivations.) The canonical variable conditions are given by

$$\langle\phi(q)|\,\hat{P}(q)\,|\phi(q)\rangle = 0, \tag{2·5}$$

$$\langle\phi(q)|\,\hat{Q}(q)\,|\phi(q)\rangle = 0, \tag{2·6}$$

$$\langle\phi(q)|\,\tilde{N}^{(\tau)}\,|\phi(q)\rangle = 0, \tag{2·7}$$

$$\langle\phi(q)|\,\hat{\Theta}^{(\tau)}(q)\,|\phi(q)\rangle = 0, \tag{2·8}$$

$$\langle\phi(q)|\,[\hat{\Theta}^{(\tau)}(q), \tilde{N}^{(\tau')}]\,|\phi(q)\rangle = i\delta_{\tau\tau'}, \tag{2·9}$$

$$\langle\phi(q)|\,[\hat{Q}(q), \hat{\Theta}^{(\tau)}(q)]\,|\phi(q)\rangle = 0, \tag{2·10}$$

$$\langle\phi(q)|\,\frac{\partial\hat{Q}}{\partial q}\,|\phi(q)\rangle = -1, \tag{2·11}$$

where $\hat{P}(q)$ is the local shift operator, defined by

$$\hat{P}(q)\,|\phi(q)\rangle = i\frac{\partial}{\partial q}\,|\phi(q)\rangle\,. \tag{2·12}$$

Differentiating (2·6) and (2·7) with respect to q and using (2·11) and (2·12), we obtain

$$\langle\phi(q)|\,[\hat{Q}(q), \hat{P}(q)]\,|\phi(q)\rangle = i, \tag{2·13}$$

$$\langle\phi(q)|\,[\tilde{N}^{(\tau)}, \hat{P}(q)]\,|\phi(q)\rangle = 0. \tag{2·14}$$

Equations (2·5), (2·6), (2·7) and (2·8) ensure that the constant terms of those operators are zero in their quasiparticle representations, while Eqs. (2·9), (2·10), (2·13) and (2·14) guarantee orthonormalization of the collective mode and the number fluctuation modes. Equation (2·11) defines the scaling of the collective coordinate.

The moving-frame HFB equation is given by

$$\delta\,\langle\phi(q)|\,\hat{H}_M(q)\,|\phi(q)\rangle = 0, \tag{2·15}$$

where

$$\hat{H}_M(q) = \hat{H} - \sum_\tau \lambda^{(\tau)}(q)\tilde{N}^{(\tau)} - \frac{\partial V}{\partial q}\hat{Q}(q) \tag{2·16}$$

represents the moving-frame Hamiltonian with the chemical potential $\lambda^{(\tau)}(q)$ and the collective potential $V(q)$ defined by

$$\lambda^{(\tau)}(q) = \frac{\partial\mathcal{H}}{\partial n^{(\tau)}}\Big|_{p=0,\boldsymbol{n}=\boldsymbol{0},\vec{I}=\vec{0}} = \langle\phi(q)|\,[\hat{H}, i\hat{\Theta}^{(\tau)}(q)]\,|\phi(q)\rangle\,, \tag{2·17}$$

$$V(q) = \mathcal{H}(q,p,\boldsymbol{n},\vec{I})\,\Big|_{p=0,\boldsymbol{n}=\boldsymbol{0},\vec{I}=\vec{0}} = \langle\phi(q)|\,\hat{H}\,|\phi(q)\rangle\,. \tag{2·18}$$

The moving-frame QRPA equations are given by

$$\delta\,\langle\phi(q)|\,[\hat{H}_M(q), i\hat{Q}(q)] - B(q)\hat{P}(q)\,|\phi(q)\rangle = 0, \tag{2·19}$$

$$\delta\,\langle\phi(q)|\,[\hat{H}_M(q), \hat{P}(q)] - iC(q)\hat{Q}(q) - \frac{1}{2B(q)}\left[\left[\hat{H}_M(q), \frac{\partial V}{\partial q}\hat{Q}(q)\right], i\hat{Q}(q)\right] - i\sum_\tau \frac{\partial\lambda^{(\tau)}}{\partial q}\tilde{N}^{(\tau)}\,|\phi(q)\rangle = 0, \tag{2·20}$$

where $B(q)$ and $C(q)$ represent the inverse collective mass and the local stiffness, respectively. They are defined by

$$B(q) = \frac{\partial^2 \mathcal{H}}{\partial p^2}\Big|_{p=0,\boldsymbol{n}=\boldsymbol{0},\vec{I}=\vec{0}} = \langle\phi(q)|\,[[\hat{H}, i\hat{Q}(q)], i\hat{Q}(q)]\,|\phi(q)\rangle\,, \tag{2·21}$$

$$C(q) = \frac{\partial^2 V}{\partial q^2} + \frac{1}{2B(q)}\frac{\partial B}{\partial q}\frac{\partial V}{\partial q}. \tag{2·22}$$

Note that the ASCC equations, (2·15), (2·19) and (2·20), are invariant under the following transformation:[56)]

$$\begin{aligned} \hat{Q}(q) &\to \hat{Q}(q) + \alpha^{(\tau)}\tilde{N}^{(\tau)}, \\ \lambda^{(\tau)}(q) &\to \lambda^{(\tau)}(q) - \alpha^{(\tau)}\frac{\partial V}{\partial q}(q), \\ \frac{\partial \lambda^{(\tau)}}{\partial q}(q) &\to \frac{\partial \lambda^{(\tau)}}{\partial q}(q) - \alpha^{(\tau)}C(q). \end{aligned} \tag{2·23}$$

Therefore, it is necessary to fix the particle number gauge for neutrons and protons in order to derive the unique solution of the ASCC equations. The algorithm to find simultaneous solutions of Eqs. (2·15), (2·19) and (2·20) satisfying the canonical variable conditions and the gauge-fixing condition is described in §4.

In this paper, we take into account the rotational motion as well as the large-amplitude vibrational motion by considering the collective Hamiltonian defined as follows:

$$\begin{aligned} \mathcal{H}(q,p,\boldsymbol{n},\vec{I}) &= \langle\phi(q,p,\boldsymbol{n})|\,\hat{H}\,|\phi(q,p,\boldsymbol{n})\rangle + \sum_{i=1}^{3}\frac{1}{2\mathcal{J}_i(q)}I_i^2 \\ &= V(q) + \frac{1}{2}B(q)p^2 + \sum_{\tau}\lambda^{(\tau)}(q)n^{(\tau)} + \sum_{i=1}^{3}\frac{1}{2\mathcal{J}_i(q)}I_i^2. \end{aligned} \tag{2·24}$$

The first and the second terms represent the potential and kinetic energies of the large-amplitude collective vibration, respectively, while the third and the fourth terms represent the energies associated with the particle-number fluctuations and the three-dimensional rotation of triaxially deformed mean fields, respectively. The three rotational moments of inertia, $\mathcal{J}_i(q)$, are defined with respect to the principal axes associated with the moving-frame HFB state $|\phi(q)\rangle$ and evaluated as

$$\delta\,\langle\phi(q)|\,[\hat{H}_M(q), \hat{\Psi}_i(q)] - \frac{1}{i}\mathcal{J}_i^{-1}(q)\hat{I}_i\,|\phi(q)\rangle = 0, \tag{2·25}$$

$$\langle\phi(q)|\,[\hat{\Psi}_i(q), \hat{I}_j]\,|\phi(q)\rangle = \delta_{ij}, \tag{2·26}$$

where $\hat{\Psi}_i(q)$ and $\hat{I}_i$ represent the rotational angle and the angular momentum operators, respectively. These equations reduce to the well-known QRPA equations giving the Thouless-Valatin moments of inertia[80)] when $|\phi(q)\rangle$ is an equilibrium state corresponding to a local minimum of the collective potential energy, $V(q)$. We call them

"Thouless-Valatin equations", although they are in fact extensions of the QRPA equations for collective rotation to non-equilibrium HFB states $|\phi(q)\rangle$. Note that $\hat{H}_M(q)$ appears in Eq. (2·25) instead of $\hat{H}$. We remark that Eqs. (2·24)–(2·26) have been introduced intuitively, leaving a full derivation of them as a challenging subject for future.

§3. Hamiltonian

We adopt the following Hamiltonian consisting of the spherical single-particle energy, the monopole and the quadrupole pairing interactions, and the quadrupole particle-hole interaction:

$$\hat{H} = \sum_k \varepsilon_k c_k^\dagger c_k - \sum_\tau \frac{G_0^{(\tau)}}{2}(\hat{A}^{(\tau)\dagger}\hat{A}^{(\tau)} + \hat{A}^{(\tau)}\hat{A}^{(\tau)\dagger}) - \sum_\tau \frac{G_2^{(\tau)}}{2} \sum_{K=-2}^{2} (\hat{B}_{2K}^{(\tau)\dagger}\hat{B}_{2K}^{(\tau)} + \hat{B}_{2K}^{(\tau)}\hat{B}_{2K}^{(\tau)\dagger}) - \frac{\chi}{2}\sum_{K=-2}^{2}\hat{D}_{2K}^\dagger \hat{D}_{2K}. \tag{3·1}$$

Here, the monopole pairing operator $\hat{A}^{(\tau)\dagger}$, the quadrupole pairing operator $\hat{B}_{2K}^{(\tau)\dagger}$, the quadrupole particle-hole operator $\hat{D}_{2K}$ are defined by

$$\hat{A}^{(\tau)\dagger} = \sum_{(k,\tilde{k})\in\tau} c_k^\dagger c_{\tilde{k}}^\dagger, \tag{3·2}$$

$$\hat{B}_{2K}^{(\tau)\dagger} = \sum_{kl\in\tau} D_{2K}^{(\tau)}(kl) c_k^\dagger c_{\tilde{l}}^\dagger, \tag{3·3}$$

$$\hat{D}_{2K} = \sum_{\tau=n,p}\sum_{kl\in\tau} D_{2K}^{(\tau)}(kl) c_k^\dagger c_l, \tag{3·4}$$

where $c_k^\dagger$ is the nucleon creation operator, and k denotes the set of quantum numbers of the single-particle state (N_k, j_k, l_k, m_k). The operator $c_{\tilde{k}}^\dagger$ represents its time-reversal state,

$$c_{\tilde{k}}^\dagger = (-1)^{j_k+m_k} c_{-k}^\dagger, \tag{3·5}$$

where the index $-k$ represents $(N_k, j_k, l_k, -m_k)$. The quadrupole matrix elements are given by

$$D_{2K}^{(\tau)}(kl) = \alpha_\tau^2 \langle k| r^2 Y_{2K} |l\rangle, \quad (kl\in\tau) \tag{3·6}$$

where the factors $\alpha_n^2 = (2N/A)^{2/3}$ and $\alpha_p^2 = (2Z/A)^{2/3}$ are multiplied to yield the same root mean square radius for neutrons and protons. For $N{=}Z$ nuclei, such as ^{68}Se and ^{72}Kr, these factors are unity. Following Baranger and Kumar,[78] we employ a model space consisting of two major oscillator shells (with the total quantum number of the lower shell denoted by N_L and that of the upper shell denoted by N_L+1), and multiply the quadrupole matrix elements $D_{2K}^{(\tau)}(kl)$ of the upper shell by the reduction factor $\zeta = (N_L+3/2)/(N_L+5/2)$.

Following the conventional prescription of the P+Q model, we ignore the Fock terms. Accordingly, we use the abbreviation "HB" in place of "HFB" in the following.

We rewrite the Hamiltonian (3·1) into the form

$$\hat{H} = \sum_k \varepsilon_k c_k^\dagger c_k - \frac{1}{2}\sum_s \kappa_s \hat{F}_s^{(+)}\hat{F}_s^{(+)} + \frac{1}{2}\sum_s \kappa_s \hat{F}_s^{(-)}\hat{F}_s^{(-)}, \tag{3·7}$$

where the Hermite operators $\hat{F}_s^{(+)}$ and the anti-Hermite operators $\hat{F}_s^{(-)}$ are defined by

$$\hat{F}_s^{(\pm)} = \frac{1}{2}(\hat{F}_s \pm \hat{F}_s^\dagger), \tag{3·8}$$

$$\begin{aligned}\hat{F}_{s=1-15} = \{&\hat{A}^{(n)}, \hat{A}^{(p)}, \hat{B}^{(n)}_{20(+)}, \hat{B}^{(n)}_{21(+)}, \hat{B}^{(n)}_{21(-)}, \hat{B}^{(n)}_{22(+)}, \hat{B}^{(n)}_{22(-)},\\ &\hat{B}^{(p)}_{20(+)}, \hat{B}^{(p)}_{21(+)}, \hat{B}^{(p)}_{21(-)}, \hat{B}^{(p)}_{22(+)}, \hat{B}^{(p)}_{22(-)}, \hat{D}_{20}, \hat{D}_{21}, \hat{D}_{22}\}.\end{aligned} \tag{3·9}$$

Here we use

$$\hat{B}^{(\tau)\dagger}_{2K(\pm)} \equiv \frac{1}{2}(\hat{B}^{(\tau)\dagger}_{2K} \pm \hat{B}^{(\tau)\dagger}_{2-K}) \quad (K \geq 0) \tag{3·10}$$

in place of $\hat{B}^{(\tau)\dagger}_{2K}$ for the quadrupole pairing operators. The interaction strengths κ_s are given by

$$\begin{aligned}\kappa_{s=1-15} = \{&2G_0^{(n)}, 2G_0^{(p)}, 2G_2^{(n)}, 4G_2^{(n)}, 4G_2^{(n)}, 4G_2^{(n)}, 4G_2^{(n)},\\ &2G_2^{(p)}, 4G_2^{(p)}, 4G_2^{(p)}, 4G_2^{(p)}, 4G_2^{(p)}, \chi, 2\chi, 2\chi\}.\end{aligned} \tag{3·11}$$

This Hamiltonian is invariant under a rotation by π about the x-axis. The quantum number associated with this is called the signature, $r = e^{-i\pi\alpha}$. The single-particle basis with definite signatures is defined by

$$\begin{aligned} d_k &\equiv \frac{1}{\sqrt{2}}(c_k + c_{\tilde{k}}), \quad r = -i \quad \left(\alpha = \frac{1}{2}\right),\\ d_{\bar{k}} &\equiv \frac{1}{\sqrt{2}}(c_{\tilde{k}} - c_k), \quad r = i \quad \left(\alpha = -\frac{1}{2}\right),\end{aligned} \tag{3·12}$$

where k denotes the single-particle basis whose magnetic quantum number satisfies the condition $m_k - 1/2 = [\text{even}]$. The operators $\hat{F}_s^{(\pm)}$ can be classified according to their signatures and K-quantum numbers, as shown in Table I.

The large-amplitude collective vibration responsible for the oblate-prolate shape mixing is associated with the $K = 0$ and 2 components of the interactions in the positive-signature ($r = +1$) sector. Thus, the infinitesimal generator of large-amplitude collective motion, $\hat{Q}(q)$, can be written in terms of the single-particle basis with definite signature as

$$\hat{Q}(q) = \sum_\tau {\sum_{kl\in\tau}}' \left(Q^{(\tau)}_{kl}(q) d_k^\dagger d_l + Q^{(\tau)}_{\bar{k}\bar{l}}(q) d_{\bar{k}}^\dagger d_{\bar{l}}\right), \tag{3·13}$$

Table I. Classification of the one-body operators $\hat{F}_s^{(\pm)}$ in terms of the signature r (or α) and K quantum numbers.

	$r=+1(\alpha=0)$	$r=-1(\alpha=1)$
$K=0$	$\{\hat{A}_n^{(\pm)}, \hat{A}_p^{(\pm)}, \hat{B}_{20(+)}^{(n)(\pm)}, \hat{B}_{20(+)}^{(p)(\pm)}, \hat{D}_{20}^{(+)}\}$	–
$K=1$	$\{\hat{B}_{21(-)}^{(n)(\pm)}, \hat{B}_{21(-)}^{(p)(\pm)}, \hat{D}_{21}^{(-)}\}$	$\{\hat{B}_{21(+)}^{(n)(\pm)}, \hat{B}_{21(+)}^{(p)(\pm)}, \hat{D}_{21}^{(+)}\}$
$K=2$	$\{\hat{B}_{22(+)}^{(n)(\pm)}, \hat{B}_{22(+)}^{(p)(\pm)}, \hat{D}_{22}^{(+)}\}$	$\{\hat{B}_{22(-)}^{(n)(\pm)}, \hat{B}_{22(-)}^{(p)(\pm)}, \hat{D}_{22}^{(-)}\}$

where $\sum'$ represents a sum over the signature pairs $(k, \bar{k})$, and $Q_{kl}^{(\tau)} = Q_{\bar{k}\bar{l}}^{(\tau)}$. The $K=1$ component of the interaction in the $r=+1$ sector and the $K=1$ and 2 components in the $r=-1$ sector contribute to the Thouless-Valatin equations (2·25).

§4. Solution of the ASCC equations for separable interactions

4.1. *The ASCC equations for separable interactions*

For the separable interactions given in (3·7), the ASCC equations are written[55),56)]

$$\delta \langle\phi(q)| \hat{h}_M(q) |\phi(q)\rangle = 0, \tag{4·1}$$

$$\delta \langle\phi(q)| [\hat{h}_M(q), \hat{Q}(q)] - \sum_s f_{Q,s}^{(-)}(q)\hat{F}_s^{(-)} - \frac{1}{i}B(q)\hat{P}(q) |\phi(q)\rangle = 0, \tag{4·2}$$

$$\begin{aligned}\delta \langle\phi(q)| &\left[\hat{h}_M(q), \frac{1}{i}B(q)\hat{P}(q)\right] - \sum_s f_{P,s}^{(+)}(q)\hat{F}_s^{(+)} - \omega^2(q)\hat{Q}(q) \\ &- \sum_s f_{R,s}^{(+)}(q)\hat{F}_s^{(+)} - \frac{1}{2}\left[\left[\hat{h}_M(q), \frac{\partial V}{\partial - q}\hat{Q}(q)\right], \hat{Q}(q)\right] \\ &+ \sum_s \left[\hat{F}_s^{(-)}, \frac{\partial V}{\partial q}\hat{Q}(q)\right] f_{Q,s}^{(-)}(q) - \sum_\tau f_N^{(\tau)}(q)\tilde{N}^{(\tau)} |\phi(q)\rangle = 0,\end{aligned} \tag{4·3}$$

where $\omega^2(q) = B(q)C(q)$ is the moving-frame QRPA frequency squared, and $\hat{h}_M(q)$ denotes the self-consistent mean-field Hamiltonian in the moving frame, defined by

$$\hat{h}_M(q) = \hat{h}(q) - \sum_\tau \lambda^{(\tau)}(q)\tilde{N}^{(\tau)} - \frac{\partial V}{\partial q}\hat{Q}(q), \tag{4·4}$$

with

$$\hat{h}(q) = \hat{h}_0 - \sum_s \kappa_s \hat{F}_s^{(+)} \langle\phi(q)| \hat{F}_s^{(+)} |\phi(q)\rangle . \tag{4·5}$$

In the above equations, the summation over s is restricted to the operators with $K=0$ and 2 in the positive-signature sector. We also define the quantities

$$f_{Q,s}^{(-)}(q) = -\kappa_s \langle\phi(q)| [\hat{F}_s^{(-)}, \hat{Q}(q)] |\phi(q)\rangle , \tag{4·6a}$$

$$f^{(+)}_{P,s}(q) = \kappa_s \langle\phi(q)| [\hat{F}^{(+)}_s, \frac{1}{i}B(q)\hat{P}(q)] |\phi(q)\rangle\,, \tag{4·6b}$$

$$f^{(+)}_{R,s}(q) = -\frac{1}{2}\kappa_s \langle\phi(q)| \left[\left[\hat{F}^{(+)}_s, \frac{\partial V}{\partial q}\hat{Q}(q)\right], \hat{Q}(q)\right] |\phi(q)\rangle\,, \tag{4·6c}$$

$$f^{(\tau)}_N(q) = B(q)\frac{\partial \lambda^{(\tau)}}{\partial q}. \tag{4·6d}$$

Note that all matrix elements are real and $\langle\phi(q)|\,\hat{F}^{(-)}_s\,|\phi(q)\rangle = 0$.

4.2. *Overview of the procedure to solve the ASCC equations*

The infinitesimal generators $\hat{Q}(q)$ and $\hat{P}(q)$, which are represented with respect to the quasiparticle vacuum $|\phi(q)\rangle$, are the solutions of the moving-frame QRPA equations, while the quasiparticle vacuum $|\phi(q)\rangle$, which depends on $\hat{Q}(q)$, is a solution of the moving-frame HB equation. In order to construct the collective path, we have to obtain a self-consistent solution for the quasiparticle vacuum and the infinitesimal generators. This requires a double iterative procedure for each value of q, because the moving-frame HB equation is also solved by iteration.

Step 0: Starting point

The shape coexistence phenomena imply that there exist several solutions of the static HB equation representing different local minima in the potential energy surface. We can choose one of the HB solutions and assume that it is on the collective path. This starting state is denoted by $|\phi(q=0)\rangle$. In the calculation for ^{68}Se and ^{72}Kr presented in this paper, we choose the HB state at the lowest minimum, which possesses an oblate shape. As discussed in Ref. 56), gauge fixing is necessary to solve the moving-frame QRPA equations. We choose the "ETOP" gauge.

Step 1: Initial setting

Assume that the solution of the ASCC equations at $q - \delta q$ is obtained. In order to calculate the solution at q, we start by solving the moving-frame HB equation (4·1). As an infinitesimal generator in the moving-frame Hamiltonian, we use an initial trial generator $\hat{Q}(q)^{(0)}$ constructed from the lowest two solutions of the moving-frame QRPA equations at $q - \delta q$ of the form

$$\hat{Q}(q)^{(0)} = (1-\varepsilon)\hat{Q}_1(q-\delta q) + \varepsilon\hat{Q}_2(q-\delta q), \tag{4·7}$$

where $\hat{Q}_1(q-\delta q)$ and $\hat{Q}_2(q-\delta q)$ denote the lowest and the second-lowest solutions of the moving-frame QRPA equations at $q-\delta q$, respectively. The mixing parameter ε is set to 0.1. This choice is crucial to find a symmetry-breaking solution in the moving-frame QRPA equations when the moving-frame HB state $|\phi(q-\delta q)\rangle$ and the moving-frame QRPA mode $\hat{Q}_1(q-\delta q)$ possess the axial symmetry.[75] [If $\hat{Q}_2(q-\delta q)$ is also axially symmetric, then we choose, for the second mode, the lowest one among the axial symmetry-breaking QRPA modes.] The quantity δq is set to 0.0157 in the present calculations.

Step 2: Solving the moving-frame HB equation

Using the operator $\hat{Q}^{(n-1)}(q)$ $(n \geq 1)$, we solve the moving-frame HB equation at q,

$$\delta \left\langle \phi^{(n)}(q) \right| \hat{H} - \sum_{\tau} (\lambda^{(\tau)}(q))^{(n)} \tilde{N}^{(\tau)} - \frac{\partial V}{\partial q}^{(n)}(q) \hat{Q}^{(n-1)}(q) \left| \phi^{(n)}(q) \right\rangle = 0, \quad (4\cdot8)$$

with three constraints from the canonical variable conditions,

$$\left\langle \phi^{(n)}(q) \right| \tilde{N}^{(\tau)} \left| \phi^{(n)}(q) \right\rangle = 0, \quad (4\cdot9)$$

$$\left\langle \phi^{(n)}(q) \right| \hat{Q}(q - \delta q) \left| \phi^{(n)}(q) \right\rangle = \delta q. \quad (4\cdot10)$$

This step is discussed in §4.3 in detail.

Step 3: Solving the moving-frame QRPA equations

Using the moving-frame HB state $\left|\phi^{(n)}(q)\right\rangle$ and the Lagrange multipliers $(\lambda^{(\tau)}(q))^{(n)}$ and $\partial V/\partial q(q)^{(n)}$ obtained in the previous step, we solve the moving-frame QRPA equations with the gauge-fixing condition used for the HB state in *Step 0*. This determines the infinitesimal generator $\hat{Q}^{(n)}(q)$ as the lowest solution of Eqs. (4·2) and (4·3). Details of this step are described in §4.4 and Appendix B.

Step 4: Realizing self-consistency

Updating the operator $\hat{Q}^{(n)}(q)$, we return to *Step 2*, and repeat *Steps 2* and *3* until all quantities at q converge.

Step 5: Progression

Change q to $q + \delta q$ and return to *Step 1*.

Carrying out *Steps 1-5*, we obtain a collective path starting from the HB minimum in one direction $(q > 0)$. We then change the sign of δq and repeat the above procedure in the opposite direction $(q < 0)$. In this way, we obtain an entire collective path.

After obtaining the solutions of the ASCC equations, we solve the Thouless-Valatin equation, (2·25), at every point on the collective path using the moving-frame HB state $|\phi(q)\rangle$ to evaluate the rotational moments of inertia $\mathcal{J}_i(q)$. Details of this calculation are described in Appendix C.

4.3. *The moving-frame HB equation in the quasiparticle representation*

The quasiparticle operators $a^\dagger_\mu(q)$ and $a_\mu(q)$ associated with the moving-frame HB state $|\phi(q)\rangle$ are written in terms of the nucleon operators, $d^\dagger_k$ and $d_{\bar{k}}$, with definite signature as

$$\begin{pmatrix} a^\dagger_\mu(q) \\ a_{\bar{\mu}}(q) \end{pmatrix} = \sum_k{}' \begin{pmatrix} U_{\mu k}(q) & V_{\mu \bar{k}}(q) \\ V_{\bar{\mu} k}(q) & U_{\bar{\mu}\bar{k}}(q) \end{pmatrix} \begin{pmatrix} d^\dagger_k \\ d_{\bar{k}}. \end{pmatrix}. \quad (4\cdot11)$$

Its inverse transformation is

$$\begin{pmatrix} d^\dagger_k \\ d_{\bar{k}} \end{pmatrix} = \sum_\mu{}' \begin{pmatrix} U_{k\mu}(q) & V_{k\bar{\mu}}(q) \\ V_{\bar{k}\mu}(q) & U_{\bar{k}\bar{\mu}}(q) \end{pmatrix} \begin{pmatrix} a^\dagger_\mu(q) \\ a_{\bar{\mu}}(q) \end{pmatrix}. \quad (4\cdot12)$$

The U and V matrices are determined by solving the moving-frame HB equation (4·1). Note that superscripts $\tau\,(=n,p)$ for U, V, and the Fermion operators are omitted for simplicity.

The moving-frame Hamiltonian is written

$$\hat{h}_M(q) = \sum_{\tau} {\sum_{kl\in\tau}}' \left((h_M^{(\tau)})_{kl}(q)(d_k^\dagger d_l + d_{\bar{k}}^\dagger d_{\bar{l}}) - \Delta_{k\bar{l}}^{(\tau)}(q)(d_k^\dagger d_{\bar{l}}^\dagger + d_{\bar{l}} d_k) \right), \tag{4·13}$$

where the particle-hole part and the particle-particle part of the moving-frame Hamiltonian are given by

$$(h_M^{(\tau)})_{ll'}(q) = h_{ll'}^{(\tau)}(q) - \lambda^{(\tau)}(q)\delta_{ll'} - \frac{\partial V}{\partial q}(q) Q_{ll'}^{(\tau)}(q), \tag{4·14}$$

$$h_{ll'}^{(\tau)} = \varepsilon_l^{(\tau)}\delta_{ll'} - \sum_{s\in ph} \kappa_s \langle\phi(q)|\, \hat{F}_s^{(+)}\, |\phi(q)\rangle\, (l|\hat{F}_s^{(+)}|l'), \tag{4·15}$$

$$\Delta_{l\bar{l}'}^{(\tau)} = \sum_{s\in pp,hh} \kappa_s \langle\phi(q)|\, \hat{F}_s^{(+)}\, |\phi(q)\rangle\, (0|\hat{F}_s^{(+)}|l\bar{l}'). \tag{4·16}$$

The matrix elements $(k|\hat{F}_s^{(+)}|l)$ are defined by

$$(l|\hat{F}_s^{(+)}|\bar{l}') = (0|d_l \hat{F}_s^{(+)} d_{\bar{l}}^\dagger|0), \quad (0|\hat{F}_s^{(+)}|l\bar{l}') = (0|\hat{F}_s^{(+)} d_l^\dagger d_{\bar{l}'}^\dagger|0), \tag{4·17}$$

where $|0)$ denotes the vacuum for nucleon operators.

The moving-frame HB equation is thus written

$${\sum_{ll'\in\tau}}' \left((h_M^{(\tau)})_{ll'}(q) U_{l'k}(q) + \Delta_{ll'}^{(\tau)}(q) V_{l'k}(q) \right) = E_k^{(\tau)} U_{lk}(q), \tag{4·18a}$$

$${\sum_{ll'\in\tau}}' \left(\Delta_{ll'}^{(\tau)}(q) U_{l'k}(q) + (h_M^{(\tau)})_{ll'}(q) V_{l'k}(q) \right) = -E_k^{(\tau)} V_{lk}(q), \tag{4·18b}$$

where $E_k^{(\tau)}$ denotes the quasiparticle energy. These equations are solved under the following three constraints:

$$\langle\phi(q)|\, \hat{N}^{(n)}\, |\phi(q)\rangle = N_0^{(n)}, \tag{4·19}$$

$$\langle\phi(q)|\, \hat{N}^{(p)}\, |\phi(q)\rangle = N_0^{(p)}, \tag{4·20}$$

$$\langle\phi(q)|\, \hat{Q}(q-\delta q)\, |\phi(q)\rangle = \delta q. \tag{4·21}$$

The Lagrange multipliers $\lambda^{(n)}(q), \lambda^{(p)}(q)$ and $dV/dq(q)$ are determined such that these constraints are satisfied. The expectation values in the moving-frame Hamiltonian are updated using U_{lk} and V_{lk} thus obtained until self-consistency is realized.

In the quasiparticle representation, the moving-frame Hamiltonian, $\hat{h}_M(q)$, the neutron and proton number operators, $\tilde{N}^{(\tau)}$, and the operators $\hat{F}_s^{(\pm)}$ with $K=0$ and 2 in the $r=1$ sector are written in the following forms:

$$\hat{h}_M(q) = \langle\phi(q)|\, \hat{h}_M(q)\, |\phi(q)\rangle + {\sum_{\mu}}' \left(E_\mu(q) \boldsymbol{B}_{\mu\mu}(q) + E_{\bar{\mu}}(q) \boldsymbol{B}_{\bar{\mu}\bar{\mu}}(q) \right), \tag{4·22}$$

$$\tilde{N}^{(\tau)} = \sum_{\mu\bar{\nu}}{}' N_A^{(\tau)}(\mu\bar{\nu})(\boldsymbol{A}^\dagger_{\mu\bar{\nu}}(q) + \boldsymbol{A}_{\mu\bar{\nu}}(q)) + \sum_{\mu}{}' N_B^{(\tau)}(\mu\mu)(\boldsymbol{B}_{\mu\mu}(q) + \boldsymbol{B}_{\bar{\mu}\bar{\mu}}(q)), \tag{4·23}$$

$$\begin{aligned}\hat{F}_s^{(\pm)} &= \langle\phi(q)|\,\hat{F}_s^{(\pm)}\,|\phi(q)\rangle + \sum_{\mu\bar{\nu}}{}' F_{A,s}^{(\pm)}(\mu\bar{\nu})(\boldsymbol{A}^\dagger_{\mu\bar{\nu}}(q) + \boldsymbol{A}_{\mu\bar{\nu}}(q)) \\ &\quad + \sum_{\mu\nu}{}' F_{B,s}^{(\pm)}(\mu\nu)(\boldsymbol{B}_{\mu\nu}(q) + \boldsymbol{B}_{\bar{\mu}\bar{\nu}}(q)),\end{aligned} \tag{4·24}$$

where

$$\boldsymbol{A}^\dagger_{\mu\bar{\nu}}(q) = a^\dagger_\mu(q)a^\dagger_{\bar{\nu}}(q), \quad \boldsymbol{A}_{\mu\bar{\nu}}(q) = a_{\bar{\nu}}(q)a_\mu(q), \quad \boldsymbol{B}_{\mu\nu}(q) = a^\dagger_\mu(q)a_\nu(q). \tag{4·25}$$

Explicit expressions for the matrix elements $N_A^{(\tau)}, N_B^{(\tau)}, F_{A,s}^{(\pm)}$ and $F_{B,s}^{(\pm)}$ are given in Appendix A.

We define the monopole-pairing gaps $\Delta_0^{(\tau)}(q)$, the quadrupole-pairing gaps $\Delta_{2,K=0,2}^{(\tau)}(q)$, and the quadrupole deformations $D_{2,K=0,2}^{(+)}(q)$ by

$$\Delta_0^{(\tau)}(q) = G_0^{(\tau)}\,\langle\phi(q)|\,\hat{A}^{(\tau)(+)}\,|\phi(q)\rangle\,, \tag{4·26}$$

$$\Delta_{2,K=0,2}^{(\tau)}(q) = G_{2,K=0,2}^{(\tau)}\,\langle\phi(q)|\,\hat{B}_{2,K=0,2(+)}^{(\tau)(+)}\,|\phi(q)\rangle\,, \tag{4·27}$$

$$D_{2,K=0,2}^{(+)}(q) = \langle\phi(q)|\,\hat{D}_{2,K=0,2}^{(+)}\,|\phi(q)\rangle\,. \tag{4·28}$$

4.4. *The moving-frame QRPA equations*

The infinitesimal generators $\hat{Q}(q)$ and $\hat{P}(q)$ are represented in the quasiparticle representation as

$$\begin{aligned}\hat{Q}(q) &= Q^A(q) + Q^B(q) \\ &= \sum_{\mu\bar{\nu}}{}' Q^A_{\mu\bar{\nu}}(q)(\boldsymbol{A}^\dagger_{\mu\bar{\nu}}(q) + \boldsymbol{A}_{\mu\bar{\nu}}(q)) + \sum_{\mu\nu}{}' Q^B_{\mu\nu}(q)(\boldsymbol{B}_{\mu\nu}(q) + \boldsymbol{B}_{\bar{\mu}\bar{\nu}}(q)),\end{aligned} \tag{4·29}$$

$$\hat{P}(q) = i\sum_{\mu\bar{\nu}}{}' P_{\mu\bar{\nu}}(q)(\boldsymbol{A}^\dagger_{\mu\bar{\nu}}(q) - \boldsymbol{A}_{\mu\bar{\nu}}(q)). \tag{4·30}$$

In the following, we discuss the method for obtaining the n-th solution of the moving-frame QRPA equations in *Step 3* assuming that the $(n-1)$-th solution $\hat{Q}^{(n-1)}(q)$ is already known. For later convenience, we introduce the one-body operator

$$\begin{aligned}\hat{R}_s^{(\pm)} &= \left[\hat{F}_s^{(\pm)}, \frac{\partial V}{\partial q}\hat{Q}^{(n-1)}(q)\right] \\ &= \langle\phi(q)|\,\hat{R}_s^{(\pm)}\,|\phi(q)\rangle + \sum_{\mu\bar{\nu}}{}' R_{A,s}^{(\pm)}(\mu\bar{\nu})(\boldsymbol{A}^\dagger_{\mu\bar{\nu}} \mp \boldsymbol{A}_{\mu\bar{\nu}}) + \sum_{\mu\nu}{}' R_{B,s}^{(\pm)}(\mu\nu)(\boldsymbol{B}_{\mu\nu} + \boldsymbol{B}_{\bar{\mu}\bar{\nu}}),\end{aligned} \tag{4·31}$$

with

$$R_{A,s}^{(\pm)}(\mu\bar{\nu}) = \frac{\partial V}{\partial q}\sum_{\rho}{}' \Big(F_{B,s}^{(\pm)}(\mu\rho)(Q^A_{\rho\bar{\nu}})^{(n-1)} \pm (Q^A_{\mu\bar{\rho}})^{(n-1)}F_{B,s}^{(\pm)}(\bar{\rho}\bar{\nu})$$

$$-(Q^B_{\mu\rho})^{(n-1)}F^{(\pm)}_{A,s}(\rho\bar{\nu}) - F^{(\pm)}_{A,s}(\mu\bar{\rho})(Q^B_{\bar{\rho}\bar{\nu}})^{(n-1)}\Big). \tag{4·32}$$

We can express the matrix elements $Q^A_{\mu\bar{\nu}}(q)$ and $P_{\mu\bar{\nu}}(q)$ using Eqs. (4·2) and (4·3) as

$$\begin{aligned}(Q^A_{\mu\bar{\nu}}(q))^{(n)} =& {\sum_{\mu'\bar{\nu}'}}' g_2(\mu\bar{\nu},\mu'\bar{\nu}')\left\{\sum_s\left(F^{(+)}_{A,s}(\mu'\bar{\nu}')f^{(+)}_{PR,s}(q) - R^{(-)}_{A,s}(\mu'\bar{\nu}')f^{(-)}_{Q,s}(q)\right)\right.\\ &\left.+\sum_\tau N^{(\tau)}(\mu'\bar{\nu}')f^{(\tau)}_N(q)\right\} + g_1(\mu\bar{\nu},\mu'\bar{\nu}')\sum_s F^{(-)}_{A,s}(\mu'\bar{\nu}')f^{(-)}_{Q,s}(q), \quad (4·33)\\ P_{\mu\bar{\nu}}(q) =& {\sum_{\mu'\bar{\nu}'}}' g_3(\mu\bar{\nu},\mu'\bar{\nu}')\left\{\sum_s\left(F^{(+)}_{A,s}(\mu'\bar{\nu}')f^{(+)}_{PR,s}(q) - R^{(-)}_{A,s}(\mu'\bar{\nu}')f^{(-)}_{Q,s}(q)\right)\right.\\ &\left.+\sum_\tau N^{(\tau)}(\mu'\bar{\nu}')f^{(\tau)}_N(q)\right\} + g_4(\mu\bar{\nu},\mu'\bar{\nu}')\sum_s F^{(-)}_{A,s}(\mu'\bar{\nu}')f^{(-)}_{Q,s}(q), \quad (4·34)\end{aligned}$$

where $f^{(+)}_{PR,s}(q) \equiv f^{(+)}_{P,s}(q) + f^{(+)}_{R,s}(q)$. The metrics $g_i\,(i = 1-4)$ are defined by

$$\begin{aligned} g_1(\mu\bar{\nu},\mu'\bar{\nu}') &\equiv (\mathcal{M}^{-1}\mathcal{E})_{\mu\bar{\nu},\mu'\bar{\nu}'}, \qquad g_2(\mu\bar{\nu},\mu'\bar{\nu}') \equiv (\mathcal{M}^{-1})_{\mu\bar{\nu},\mu'\bar{\nu}'}, \quad (4·35)\\ g_3(\mu\bar{\nu},\mu'\bar{\nu}') &\equiv (\mathcal{E}\mathcal{M}^{-1})_{\mu\bar{\nu},\mu'\bar{\nu}'}, \qquad g_4(\mu\bar{\nu},\mu'\bar{\nu}') \equiv (\mathcal{E}\mathcal{M}^{-1}\mathcal{E})_{\mu\bar{\nu},\mu'\bar{\nu}'} - \delta_{\mu\mu'}\delta_{\bar{\nu}\bar{\nu}'}, \quad (4·36)\end{aligned}$$

where $\mathcal{M}$ and $\mathcal{E}$ are given by

$$\begin{aligned}\mathcal{M}_{\mu\bar{\nu},\mu'\bar{\nu}'}(\omega^2(q)) =& \{(E_\mu + E_{\bar{\nu}})^2 - \omega^2(q)\}\delta_{\mu\mu'}\delta_{\bar{\nu}\bar{\nu}'}\\ &+ \delta_{\mu\mu'}\left(\frac{1}{2}E_{\mu'} + E_{\nu'} - \frac{1}{2}E_{\bar{\nu}}\right)(Q^B_{\nu'\bar{\nu}})^{(n-1)}\frac{\partial V}{\partial q}(q),\\ &+ (Q^B_{\mu\mu'})^{(n-1)}\left(E_{\mu'} - \frac{1}{2}E_\mu + \frac{1}{2}E_{\bar{\nu}'}\right)\delta_{\bar{\nu}\bar{\nu}'}\frac{\partial V}{\partial q}(q), \quad (4·37)\\ \mathcal{E}_{\mu\bar{\nu},\mu'\bar{\nu}'} =& (E_\mu + E_{\bar{\nu}})\delta_{\mu\mu'}\delta_{\bar{\nu}\bar{\nu}'}. \quad (4·38)\end{aligned}$$

The quantities given in (4·6) and the canonical variable condition (2·14) can be expressed in terms of $(\hat{Q}^A(q))^{(n)}$ and $\hat{P}(q)$ as

$$\begin{aligned} f^{(-)}_{Q,s}(q) =& -\kappa_s\langle\phi(q)|\,[\hat{F}^{(-)}_s, \hat{Q}^{(n)}(q)]\,|\phi(q)\rangle = -2\kappa_s(F^{(-)}_{A,s}, (Q^A(q))^{(n)}), \quad (4·39)\\ f^{(+)}_{PR,s}(q) =& \kappa_s\langle\phi(q)|\,[\hat{F}^{(+)}_s, \frac{1}{i}B(q)\hat{P}(q)]\,|\phi(q)\rangle\\ &-\frac{1}{2}\kappa_s\langle\phi(q)|\left[\left[\hat{F}^{(+)}_s, \frac{\partial V}{\partial q}\hat{Q}^{(n-1)}(q)\right], \hat{Q}^{(n)}(q)\right]|\phi(q)\rangle\\ =& 2\kappa_s(F^{(+)}_{A,s}, P(q)) - \kappa_s(R^{(+)}_{A,s}, (Q^A(q))^{(n)}), \quad (4·40)\end{aligned}$$

$$\langle\phi(q)|\,[\hat{N}^{(\tau)}, \hat{P}(q)]\,|\phi(q)\rangle = -2i(N^{(\tau)}_A, P(q)) = 0, \tag{4·41}$$

where

$$(X,Y) \equiv \sum_{\mu\bar{\nu}}{}' X(\mu\bar{\nu})Y(\mu\bar{\nu}). \tag{4·42}$$

Substituting Eqs. (4·39), (4·40) and (4·41) into Eqs. (4·33) and (4·34), we derive the dispersion equation

$$\boldsymbol{S}\cdot\boldsymbol{f} = \sum_{s'\tau'} \begin{pmatrix} S^{Q,Q}_{ss'} & S^{Q,PR}_{ss'} & S^{Q,N}_{s\tau'} \\ S^{PR,Q}_{ss'} & S^{PR,PR}_{ss'} & S^{PR,N}_{s\tau'} \\ S^{N,Q}_{\tau s'} & S^{N,PR}_{\tau s'} & S^{N,N}_{\tau\tau'} \end{pmatrix} \begin{pmatrix} f^{(-)}_{Q,s'}(q) \\ f^{(+)}_{PR,s'}(q) \\ f^{(\tau')}_{N}(q) \end{pmatrix} = 0, \tag{4·43}$$

where the matrix elements of $\boldsymbol{S}$ are given by

$$\begin{aligned}
S^{Q,Q}_{ss'} &= 2(F^{(-)}_{A,s}, F^{(-)}_{A,s'})_{g_1} - 2(F^{(-)}_{A,s}, R^{(-)}_{A,s'})_{g_2} - \frac{1}{\kappa_s}\delta_{ss'}, && (4·44a)\\
S^{Q,PR}_{ss'} &= 2(F^{(-)}_{A,s}, F^{(+)}_{A,s'})_{g_2}, && (4·44b)\\
S^{Q,N}_{s\tau'} &= 2(F^{(-)}_{A,s}, N^{(\tau')}_{A})_{g_2}, && (4·44c)\\
S^{PR,Q}_{ss'} &= 2(F^{(+)}_{A,s}, F^{(-)}_{A,s'})_{g_4} - 2(F^{(+)}_{A,s}, R^{(-)}_{A,s'})_{g_3} \\
&\quad + (R^{(+)}_{A,s}, F^{(-)}_{A,s'})_{g_1} - (R^{(+)}_{A,s}, R^{(-)}_{A,s'})_{g_2}, && (4·44d)\\
S^{PR,PR}_{ss'} &= 2(F^{(+)}_{A,s}, F^{(+)}_{A,s'})_{g_3} + (R^{(+)}_{A,s}, F^{(+)}_{A,s'})_{g_2} - \frac{1}{\kappa_s}\delta_{ss'}, && (4·44e)\\
S^{PR,N}_{s\tau'} &= 2(F^{(+)}_{A,s}, N^{(\tau')}_{A})_{g_3} + (R^{(+)}_{A,s}, N^{(\tau')}_{A})_{g_2}, && (4·44f)\\
S^{N,Q}_{\tau s'} &= (N^{(\tau)}_{A}, F^{(-)}_{A,s'})_{g_4} - (N^{(\tau)}_{A}, R^{(-)}_{A,s'})_{g_3}, && (4·44g)\\
S^{N,PR}_{\tau s'} &= (N^{(\tau)}_{A}, F^{(+)}_{A,s'})_{g_3}, && (4·44h)\\
S^{N,N}_{\tau\tau'} &= (N^{(\tau)}_{A}, N^{(\tau')}_{A})_{g_3}. && (4·44i)
\end{aligned}$$

The parentheses in the above matrix elements are defined by

$$(X,Y)_{g_i} = \sum_{\mu\bar{\nu}\mu'\bar{\nu'}}{}' X(\mu\bar{\nu})g_i(\mu\bar{\nu}\mu'\bar{\nu'})Y(\mu'\bar{\nu'}). \quad (i=1-4) \tag{4·45}$$

As mentioned above, the ASCC equations are invariant under the gauge transformation associate with number fluctuations. The quantities

$$f^{(-)}_{Q,s=1,2}(q) = -2G_0^{(\tau=n,p)} \langle\phi(q)|\,[\hat{A}^{(\tau=n,p)(-)}, \hat{Q}(q)]\,|\phi(q)\rangle \tag{4·46}$$

and $f^{(\tau)}_N(q)$ are transformed under (2·23) as

$$\begin{aligned}
f^{(-)}_{Q,s=1,2}(q) &\to f^{(-)}_{Q,s=1,2}(q) - 4\alpha^{(\tau=n,p)}\Delta_0^{(\tau=n,p)}(q), && (4·47)\\
f^{(\tau=n,p)}_{N}(q) &\to f^{(\tau=n,p)}_{N}(q) - \alpha^{(\tau=n,p)}\omega^2(q). && (4·48)
\end{aligned}$$

Thus, we have to fix the gauge when solving the dispersion equation (4·43). For both neutrons and protons, we choose the "ETOP" gauge,[56]

$$f^{(-)}_{Q,s=1}(q) = 0, \quad f^{(-)}_{Q,s=2}(q) = 0. \tag{4·49}$$

This gauge-fixing condition reduces the dimension of the dispersion equations. We can then use the submatrix $\boldsymbol{S'}$ of $\boldsymbol{S}$, where terms related to the anti-Hermite part of the monopole pairing operators, $(\hat{F}^{(-)}_{s=1,2})$, are dropped. From Eq. (4·43), the moving-frame QRPA frequency squared, $\omega^2(q)$, is determined by the condition

$$\det \boldsymbol{S'}(\omega^2(q)) = 0. \tag{4·50}$$

The solution with the smallest value of $\omega^2(q)$ (including negative values) is regarded as the most collective mode at q. Note that we consider imaginary $\omega(q)$ solutions as well as real ones. Once $\omega^2(q)$ is determined, $\boldsymbol{f}(q)$, $(Q^A_{\mu\bar{\nu}}(q))^{(n)}$ and $P_{\mu\bar{\nu}}(q)$ can be obtained by use of the normalization condition

$$\langle\phi(q)|\,[(\hat{Q}^A(q))^{(n)}, \hat{P}(q)]\,|\phi(q)\rangle = 2i((Q^A(q))^{(n)}, P(q)) = i. \tag{4·51}$$

§5. Requantization of the collective Hamiltonian

5.1. *Requantization and construction of wave functions in the laboratory frame*

Solving the basic equations of the ASCC method and the Thouless-Valatin equations, we obtain the collective Hamiltonian (2·24); we can set the collective mass $B(q)^{-1}$ to unity without loss of generality, because it merely defines the scale for measuring the length of the collective path. We also set the number fluctuation $\boldsymbol{n}$ to zero. Requantization is carried out simply by replacing the classical variables with the quantum operators:

$$p \to \frac{\hbar}{i}\frac{\partial}{\partial q}, \quad I_i \to \hat{I}_i, \tag{5·1}$$

where $\hat{I}_i$ are three components of the angular momentum operator acting on three Euler angles that define the orientation of the principal axes with respect to the laboratory frame. The Schrödinger equation for the requantized collective Hamiltonian is

$$\left(-\frac{1}{2}\frac{\partial^2}{\partial q^2} + \sum_{i=1}^{3}\frac{\hat{I}_i^2}{2\mathcal{J}_i(q)} + V(q)\right)\Psi_{IMk}(q,\Omega) = E_{I,k}\Psi_{IMk}(q,\Omega). \tag{5·2}$$

The collective wave function in the laboratory frame, $\Psi_{IM,k}(q,\Omega)$, is a function of the collective coordinate q and the three Euler angles Ω, and it is specified by the total angular momentum I, its projection M on the laboratory z-axis, and the index k distinguishing different quantum states having the same I and M. Note that the three components $\hat{I}_i$ of the angular momentum operator are defined with respect to the principal axes $(1,2,3) \equiv (x',y',z')$ associated with the moving-frame HB state $|\phi(q)\rangle$.

Using the rotational wave functions $\mathscr{D}^I_{MK}(\Omega)$, we can write the collective wave functions in the laboratory frame as

$$\Psi_{IMk}(q,\Omega) = \sum_{K=-I}^{I} \Phi'_{IKk}(q)\sqrt{\frac{2I+1}{8\pi^2}}\mathscr{D}^I_{MK}(\Omega) \tag{5·3}$$

$$= \sum_{K=0}^{I} \Phi_{IKk}(q)\,\langle\Omega|IMK\rangle\,. \tag{5·4}$$

Here, Φ'_{IKk} are intrinsic wave functions that represent the large-amplitude collective vibrations responsible for the oblate-prolate shape mixing. They are specified by the projection K of the angular momentum on the intrinsic z'-axis, instead of by M. We assume that the intrinsic states have positive signature. Then, their K and $-K$ components are connected by

$$\Phi'_{IKk}(q) = (-)^I\Phi'_{I-Kk}(q). \tag{5·5}$$

Accordingly, it is convenient to use new rotational wave functions, defined by

$$\langle\Omega|IMK\rangle = \frac{1}{\sqrt{2(1+\delta_{K0})}}\sqrt{\frac{2I+1}{8\pi^2}}\left(\mathscr{D}^I_{MK}(\Omega) + (-)^I\mathscr{D}^I_{M-K}(\Omega)\right), \tag{5·6}$$

and new vibrational wave functions,

$$\Phi_{IKk}(q) = \sqrt{\frac{2}{1+\delta_{K0}}}\Phi'_{IKk}(q) = (-)^I\sqrt{\frac{2}{1+\delta_{K0}}}\Phi'_{I-Kk}(q), \tag{5·7}$$

in place of $\Phi'_{IK,k}$. Because the $\mathscr{D}$ functions are normalized as

$$\int d\Omega\mathscr{D}^{I*}_{MK}(\Omega)\mathscr{D}^{I'}_{M'K'}(\Omega) = \frac{8\pi^2}{2I+1}\delta_{II'}\delta_{MM'}\delta_{KK'}, \tag{5·8}$$

the normalization of the vibrational wave functions is given by

$$\int dq \sum_{K=0}^{I} \Phi^*_{IKk}(q)\Phi_{IKk'}(q) = \delta_{kk'}. \tag{5·9}$$

5.2. *Boundary conditions*

Multiplying the Schrödinger equation (5·2) from the left by a rotational wave function $\langle\Omega|IMK\rangle$ and integrating out the Euler angles Ω, we obtain the collective Schrödinger equation for large-amplitude vibration:

$$\left(-\frac{1}{2}\frac{\partial^2}{\partial q^2} + V(q)\right)\Phi_{IKk}(q) + \sum_{K'=0}^{I}\langle IMK|\,\hat{T}_{\rm rot}\,\big|IMK'\big\rangle\,\Phi_{IK'k}(q) = E_{I,k}\Phi_{IKk}(q), \tag{5·10}$$

where $\hat{T}_{\rm rot} = \sum_i \hat{I}_i^2/(2\mathcal{J}_i(q))$.

The boundary conditions can be specified by projecting the collective path onto the (β, γ) plane and by using the well-known symmetry properties of the Bohr-Mottelson collective Hamiltonian.[5),79)] The deformation parameters β and γ are defined by

$$\beta(q)\cos\gamma(q) = \chi' \langle\phi(q)|\, \hat{D}^{(+)}_{20}\, |\phi(q)\rangle /(\hbar\omega_0 b^2), \tag{5·11}$$

$$\beta(q)\sin\gamma(q) = \sqrt{2}\chi' \langle\phi(q)|\, \hat{D}^{(+)}_{22}\, |\phi(q)\rangle /(\hbar\omega_0 b^2), \tag{5·12}$$

and they measure the magnitude and triaxiality of the quadrupole deformation of the HB mean field in the moving-frame as functions of the collective coordinate q. Here, $\hbar\omega_0$ denotes the frequency of the harmonic-oscillator potential, $\chi' \equiv \chi b^4$, and the harmonic-oscillator length parameter b is related to the radius parameter r_0 by

$$b^2 = \frac{4}{5}\left(\frac{2}{3}\right)^{\frac{1}{3}} r_0^2 A^{\frac{1}{3}}. \tag{5·13}$$

The boundary conditions for the vibrational collective wave functions are specified according to the form of the collective path in the (β, γ) plane. As we discuss in §6.3, the collective path for ^{68}Se passes through the γ-direction (see Fig.1). In this case, the following boundary conditions are employed in the prolate and oblate limits. In the prolate limit, $\gamma(q_{\rm pro}) \to 0°$, the vibrational wave functions must satisfy

$$\Phi_{IKk}(q_{\rm pro} - q) = (-)^{\frac{K}{2}} \Phi_{IKk}(q_{\rm pro} + q), \tag{5·14}$$

which is equivalent to

$$\Phi_{IKk}(q_{\rm pro}) = 0, \quad (K = 2, 6, \cdots) \tag{5·15}$$

$$\left.\frac{d\Phi_{IKk}}{dq}\right|_{q=q_{\rm pro}} = 0. \quad (K = 0, 4, \cdots) \tag{5·16}$$

In the oblate limit, $\gamma(q_{\rm ob}) \to 60°$, the HB mean field is symmetric about the intrinsic y'-axis, and thus the boundary conditions are given by[79)]

$$\Phi_{IKk}(q_{\rm ob} - q) = (-)^{\frac{K}{2}} \sum_{K'} \frac{2}{\sqrt{(1+\delta_{K0})(1+\delta_{K'0})}} \mathscr{D}^I_{KK'}\left(\frac{\pi}{2}, \frac{\pi}{2}, \pi\right) \Phi_{IK'k}(q_{\rm ob} + q). \tag{5·17}$$

In the case of ^{72}Kr, the collective path connecting the oblate and prolate shapes is not periodic with respect to the γ-direction (see Fig. 3). Accordingly, we set the box boundary conditions at the edge of the path:

$$\Phi_{IKk}(q_{\rm min}) = \Phi_{IKk}(q_{\rm max}) = 0. \tag{5·18}$$

The matrix elements $\langle IMK|\, \hat{T}_{\rm rot}\, |IMK'\rangle$ of the rotational kinetic energy operator in Eq. (5·10) can be easily calculated:

$$\langle IMK|\, \hat{T}_{\rm rot}\, |IMK\rangle = a(q)I(I+1) + b(q)K^2, \tag{5·19}$$

$$\begin{aligned}\langle IMK|\, \hat{T}_{\rm rot}\, |IM, K+2\rangle &= \langle IM, K+2|\, \hat{T}_{\rm rot}\, |IMK\rangle \\ &= c(q)\{(I+K+2)(I+K+1)(I-K)(I-K-1)\}^{-\frac{1}{2}},\end{aligned} \tag{5·20}$$

where

$$a(q) = \frac{1}{4}\left(\frac{1}{\mathcal{J}_1(q)} + \frac{1}{\mathcal{J}_2(q)}\right), \tag{5·21}$$

$$b(q) = \frac{1}{4}\left(\frac{2}{\mathcal{J}_3(q)} - \frac{1}{\mathcal{J}_1(q)} - \frac{1}{\mathcal{J}_2(q)}\right), \tag{5·22}$$

$$c(q) = \frac{1}{8}\left(\frac{1}{\mathcal{J}_1(q)} - \frac{1}{\mathcal{J}_2(q)}\right). \tag{5·23}$$

The other matrix elements are zero.

5.3. *Electric quadrupole moments and transitions*

To evaluate the electric quadrupole (E2) moments and transition probabilities, we need to derive expressions for the E2 operator in the collective subspace. This can be easily done by using the procedure we used to derive the quantum collective Hamiltonian. As described below, we first evaluate the expectation values of the E2 operators with respect to the moving-frame HB state $|\phi(q,p)\rangle$ and then apply the canonical quantization procedure.

In accordance with the quadrupole operators (3·4), we define the E2 operators in the model space under consideration as

$$\hat{D}'^{(\mathrm{E2})}_{\mu} = \sum_{\tau} e^{(\tau)}_{\mathrm{eff}} \sum_{kl\in\tau} D^{(\tau)}_{2\mu}(kl) c^{\dagger}_{k} c_{l}, \tag{5·24}$$

$$\hat{D}'^{(\mathrm{E2})}_{\mu+} = \frac{1}{2}(\hat{D}'^{(\mathrm{E2})}_{\mu} + \hat{D}'^{(\mathrm{E2})}_{-\mu}), \tag{5·25}$$

where $e^{(\tau)}_{\mathrm{eff}}$ are the effective charges. Their expectation values in the collective subspace are expanded up to second order in the collective momentum p as

$$\begin{aligned} D'^{(\mathrm{E2})}_{\mu+}(q,p) &= \langle\phi(q,p)|\, \hat{D}'^{(\mathrm{E2})}_{\mu+}\, |\phi(q,p)\rangle \\ &= D'^{(\mathrm{E2})}_{\mu+}(q) + \frac{1}{2} D''^{(\mathrm{E2})}_{\mu+}(q) p^2, \end{aligned} \tag{5·26}$$

where

$$D'^{(\mathrm{E2})}_{\mu+}(q) = \langle\phi(q)|\, \hat{D}'^{(\mathrm{E2})}_{\mu+}\, |\phi(q)\rangle\,, \tag{5·27}$$

$$D''^{(\mathrm{E2})}_{\mu+}(q) = -\,\langle\phi(q)|\, [[\hat{D}'^{(\mathrm{E2})}_{\mu+}, \hat{Q}(q)], \hat{Q}(q)]\, |\phi(q)\rangle\,. \tag{5·28}$$

The quantities $D'^{(\mathrm{E2})}_{\mu+}(q,p)$ are called collective representations of the E2 operators. Note that these are defined in the intrinsic frame associated with the moving-frame HB mean field. We now apply the canonical quantization to them. Then, the collective coordinate q and the collective momentum p become quantum operators acting on the vibrational wave functions $\Phi_{IKk}(q)$. We call the requantized E2 operators "collective E2 operators" and denote them $\hat{D}'^{(\mathrm{E2})}_{\mu+}$. Thus, the E2 matrix elements between two collective vibrational states are evaluated as

$$\langle\Phi_{IKk}|\, \hat{D}'^{(\mathrm{E2})}_{\mu+}\, |\Phi_{IK'k'}\rangle = \int dq\, \Phi^{*}_{IKk}(q) \left(D'^{(\mathrm{E2})}_{\mu+}(q) - \frac{1}{2}\frac{d}{dq} D''^{(\mathrm{E2})}_{\mu+}(q) \frac{d}{dq}\right) \Phi_{IK'k'}(q). \tag{5·29}$$

We need to calculate these integrals only for vibrational states which satisfy the selection rules of the E2 operators. (As shown in §6, the contribution from the second term in the r.h.s. of Eq. (5·29) is negligible, so that the ordering problem in the canonical quantization procedure is not important here.)

The collective E2 operators $\hat{D}'^{(\mathrm{E2})}_{\mu}$ are defined in the intrinsic frame, and those in the laboratory frame $\hat{D}^{(\mathrm{E2})}_{\mu}$ are obtained as

$$\hat{D}^{(\mathrm{E2})}_{\mu} = \sum_{\mu} \mathscr{D}^{2}_{\mu\mu'}(\Omega)\hat{D}'^{(\mathrm{E2})}_{\mu'}. \tag{5·30}$$

As is well known, $B(\mathrm{E2})$ values and spectroscopic quadrupole moments $Q(Ik)$ are given in terms of reduced matrix elements $\langle Ik||\hat{D}^{(\mathrm{E2})}_{+}||Ik\rangle$ as

$$B(\mathrm{E2}; Ik \to I'k') = (2I+1)^{-1}\left|\langle Ik||\hat{D}^{(\mathrm{E2})}||I'k'\rangle\right|^2, \tag{5·31}$$

$$\begin{aligned} Q(Ik) &= \sqrt{\frac{16\pi}{5}}\,\langle I, M=I, k|\,\hat{D}^{(\mathrm{E2})}\,|I, M=I, k\rangle \\ &= \sqrt{\frac{16\pi}{5}}\begin{pmatrix} I & 2 & I \\ -I & 0 & I \end{pmatrix}\langle Ik||\hat{D}^{(\mathrm{E2})}_{\mu}||Ik\rangle. \end{aligned} \tag{5·32}$$

These reduced matrix elements can be evaluated by using the Wigner-Eckart theorem,

$$\langle I, M=I, k|\,\hat{D}^{(\mathrm{E2})}_{0}\,\big|I', M=I, k'\big\rangle = \begin{pmatrix} I & 2 & I' \\ -I & 0 & I \end{pmatrix}\langle I, k||\hat{D}^{(\mathrm{E2})}||I', k'\rangle, \tag{5·33}$$

and calculating the left-hand side as[79]

$$\begin{aligned} &\langle I, M=I, k|\hat{D}^{(\mathrm{E2})}_{0}\,\big|I', M=I, k'\big\rangle \\ &\quad= \frac{\sqrt{(2I+1)(2I'+1)}}{8\pi^2}\sum_{KK'\mu}\left\langle \Phi'_{IKk}\right|\hat{D}'^{(\mathrm{E2})}_{\mu}\left|\Phi'_{I'K'k'}\right\rangle\left\langle \mathscr{D}^{I}_{IK}\right|\mathscr{D}^{2}_{0\mu}\left|\mathscr{D}^{I'}_{IK'}\right\rangle \\ &\quad= \sqrt{(2I+1)(2I'+1)}\sum_{KK'\mu}\left\langle \Phi'_{IKk}\right|\hat{D}'^{(\mathrm{E2})}_{\mu}\left|\Phi'_{I'K'k'}\right\rangle \\ &\qquad (-)^{I-K}\begin{pmatrix} I & 2 & I' \\ -I & 0 & I \end{pmatrix}\begin{pmatrix} I & 2 & I' \\ -K & \mu & K' \end{pmatrix}. \end{aligned} \tag{5·34}$$

In the intrinsic frame, the $\mu = \pm 1$ components of the collective E2 operator vanish, and those for the $\mu = \pm 2$ components are equal. Thus we obtain

$$\begin{aligned} &\langle Ik||\hat{D}^{(\mathrm{E2})}||I'k'\rangle \\ &\quad= \sqrt{(2I+1)(2I'+1)}(-)^{I}\sum_{K\geq 0}\left[\begin{pmatrix} I & 2 & I' \\ -K & 0 & K \end{pmatrix}\langle \Phi_{IKk}|\,\hat{D}'^{(\mathrm{E2})}_{0+}\,|\Phi_{I'K'k'}\rangle\right. \\ &\qquad + \sqrt{1+\delta_{K0}}\left\{\begin{pmatrix} I & 2 & I' \\ -K-2 & 2 & K \end{pmatrix}\langle \Phi_{I,K+2,k}|\,\hat{D}'^{(\mathrm{E2})}_{2+}\,|\Phi_{I'Kk'}\rangle\right. \\ &\qquad \left.\left. + \begin{pmatrix} I & 2 & I' \\ K & 2 & -K-2 \end{pmatrix}(-)^{I+I'}\left\langle \Phi_{IKk}\right|\hat{D}'^{(\mathrm{E2})}_{2+}\left|\Phi_{I',K+2,k'}\right\rangle\right\}\right]. \end{aligned} \tag{5·35}$$

§6. Results of numerical calculation and discussion

6.1. *Details of numerical calculation*

In the numerical calculations, we considered two major shells ($N_{\rm sh} = 3, 4$) for protons and neutrons and used the same values for the single-particle energies, the monopole pairing strength $G_0^{(\tau)}$, and the quadrupole particle-hole interaction strength χ as in Ref. 75). The single-particle energies are listed in Table II. The interaction strengths were adjusted to approximately reproduce the pairing gaps and the quadrupole deformations obtained with the Skyrme-HFB calculation carried out by Yamagami et al.[67] These values are $G_0^{(n)} = G_0^{(p)} = 0.320$ and $\chi' \equiv \chi b^4 = 0.248$ MeV for ^{68}Se and $G_0^{(n)} = 0.299, G_0^{(p)} = 0.309$ and $\chi' = 0.255$ MeV for ^{72}Kr. The oscillator frequency and the radius parameters were set to $\hbar\omega_0 = 41.2A^{1/3}$ MeV and $r_0 = 1.2$ fm. For the quadrupole pairing strength, we used the self-consistent value derived by Sakamoto and Kishimoto,[82]

$$G_{2K}^{(\tau)\rm self} = \left[\sum_{\alpha\beta\in\tau} \frac{1}{4} \left(\frac{1}{E_\alpha} + \frac{1}{E_\beta} \right) |D_{2K}^{(\tau)}(\alpha\beta)|^2 \right]^{-1}, \tag{6·1}$$

where E_α is the quasiparticle energy evaluated using the BCS approximation in the case of spherical shape. Accordingly, we have $G_{20}^{\rm self} = G_{21}^{\rm self} = G_{22}^{\rm self}$.

The effective charges $e_{\rm eff}^{(\tau)}$ are written as $e_{\rm eff}^{(n)} = \delta e_{\rm pol}$ for neutrons and $e_{\rm eff}^{(p)} = e + \delta e_{\rm pol}$ for protons. For simplicity, we use the same polarization charge, $\delta e_{\rm pol} = 0.905e$, for protons and neutrons, which is chosen to reproduce the experimental $B(\mathrm{E2};2_1^+ \to 0_1^+)$ value[66] in ^{72}Kr. Only these data are available for E2 transitions among low-lying states in ^{68}Se and ^{72}Kr. This value of $\delta e_{\rm pol}$ seems slightly too large and needs further investigation. We take into account the momentum-dependent term in the collective representation of the E2 operators, Eq. (5·26), although numerical calculations indicate that it gives only a few percent correction, at most, to the main term.

In the present calculation, we ignored the curvature terms [the fourth, fifth and sixth terms in Eq. (4·3)] in order to reduce the CPU time. We have verified that their contributions are negligible.

In the numerical calculations, careful treatment is necessary in the prolate limit, as the moment of inertia about the symmetry axis, $\mathcal{J}_3(q)$, vanishes there. Actually, this does not cause a problem, because the $K \neq 0$ components of the vibrational wave function also vanish there. To avoid numerical instability, however, we set $\mathcal{J}_3(q) = 10^{-13}\hbar^2$ (MeV)$^{-1}$ in the prolate limit, and we confirmed that this works well without losing numerical accuracy. We applied this recipe also in the oblate limit, where $\mathcal{J}_2(q)$ vanishes. Actually, the y'-axis component of the vibrational wave function also vanishes there, although this is not directly seen from Eq. (5·10), in which the wave functions are decomposed with respect to the K quantum numbers, choosing the z'-axis as the quantization axis.

Table II. Energies in units of MeV of the spherical single-particle levels used in the calculation. These values are taken from Ref. 75).

orbits	$1f_{7/2}$	$2p_{3/2}$	$1f_{5/2}$	$2p_{1/2}$	$1g_{9/2}$	$2d_{5/2}$	$1g_{7/2}$	$3s_{1/2}$	$2d_{3/2}$
neutrons	−9.02	−4.93	−2.66	−2.21	0.00	5.27	6.36	8.34	8.80
protons	−8.77	−4.23	−2.41	−1.50	0.00	6.55	5.90	10.10	9.83

6.2. *Properties of local minima in ^{68}Se and ^{72}Kr*

In Table III we list the results of the calculations for the properties of the HB equilibrium states (local minima in the potential energy surface). For both ^{68}Se and ^{72}Kr, the lowest HB minimum possesses an oblate shape, while the second minimum is prolate. The energy differences between the oblate and prolate minima evaluated using the P+Q Hamiltonian with (without) the quadrupole pairing interaction are 300 keV (196 keV) for ^{68}Se and 827 keV (626 keV) for ^{72}Kr. We thus find no qualitative change in the mean-field properties due to the inclusion of the quadrupole pairing interaction.

The QRPA collective modes at the oblate and prolate minima can be classified in terms of the projections of the angular momenta on the symmetry axis, K_y and $K_z \equiv K$, respectively. Table IV lists the properties of the QRPA collective modes at the oblate and prolate minima. In ^{68}Se, the lowest modes are γ-vibrational (K_y or K_z=2), and the second lowest modes are β-vibrational (K_y or K_z=0), both at the oblate and the prolate minima. It is seen that the quadrupole pairing interaction lowers their excitation energies without changing their ordering. In ^{72}Kr, the lowest QRPA modes at the two minima are both β-vibrational if the quadrupole pairing interaction is ignored. Note, however, that the $K_z = 0$ and 2 modes at the prolate local minimum are close in energy, and their ordering changes when the quadrupole pairing interaction is taken into account, whereas the lowest mode at the lowest oblate minimum is always β-vibrational.

6.3. *Collective path connecting the oblate and prolate minima in ^{68}Se*

We start by solving the basic equations of the ASCC method from the oblate minimum ($q = 0$) and progressively determine the collective path, following the algorithm outlined in §4.2. Figure 1 illustrates the collective path thus obtained by projecting it onto the (β, γ) potential energy surface. The path connects the two local minima passing through a potential valley lying in the triaxial deformed region. The

Table III. The quadrupole deformations and the pairing gaps $\Delta_0^{(\tau)}$ (in MeV) and $\Delta_{2K}^{(\tau)}$ (in MeV fm^2) at the HB local minima in ^{68}Se and ^{72}Kr, calculated using the P+Q Hamiltonian, including the quadrupole pairing interaction.

$(G_2 = G_2^{\rm self})$	β	γ	$\Delta_0^{(n)}$	$\Delta_0^{(p)}$	$\Delta_{20}^{(n)}$	$\Delta_{20}^{(p)}$	$\Delta_{22}^{(n)}$	$\Delta_{22}^{(p)}$
^{68}Se (oblate)	0.30	60°	1.17	1.26	0.08	0.09	0.10	0.11
^{68}Se (prolate)	0.26	0°	1.34	1.40	0.14	0.15	0	0
^{72}Kr (oblate)	0.35	60°	0.92	1.06	0.05	0.06	0.06	0.07
^{72}Kr (prolate)	0.38	0°	1.14	1.27	0.19	0.19	0	0

Table IV. The excitation energies ω (in MeV) and the K quantum numbers of the lowest two QRPA modes at the oblate and prolate minima in ^{68}Se and ^{72}Kr. The results of the calculation with ($G_2 = G_2^{\rm self}$) and without ($G_2 = 0$) the quadrupole pairing interaction are compared. The K quantum numbers here represent K_y or K_z, according to the shape (oblate or prolate).

	$G_2 = 0$				$G_2 = G_2^{\rm self}$			
	ω_1	K_1	ω_2	K_2	ω_1	K_1	ω_2	K_2
^{68}Se (oblate)	1.555	2	2.342	0	1.373	2	2.131	0
^{68}Se (prolate)	1.015	2	1.915	0	0.898	2	1.369	0
^{72}Kr (oblate)	1.150	0	1.909	0	1.239	0	2.010	2
^{72}Kr (prolate)	1.606	0	1.674	2	1.644	2	1.714	0

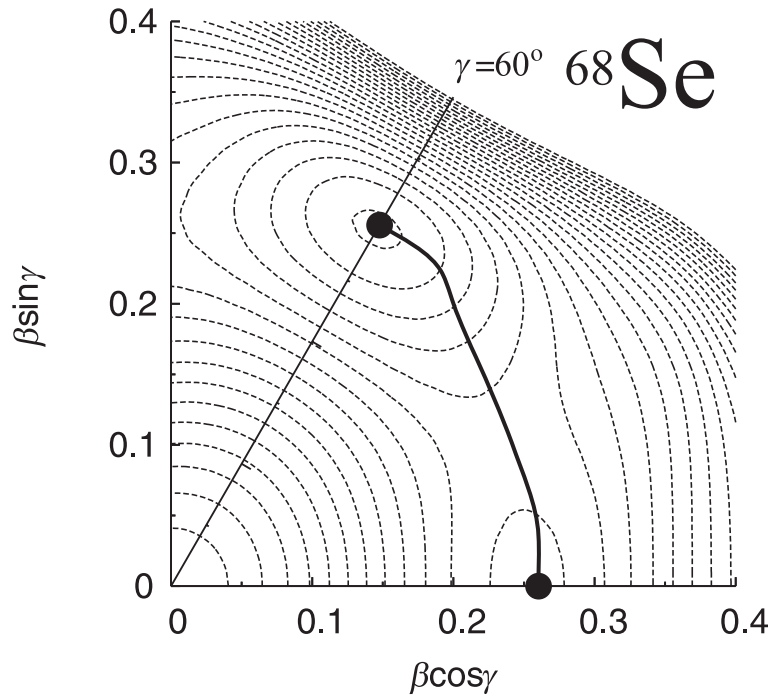

Fig. 1. The collective path for ^{68}Se calculated with the P+Q Hamiltonian including the quadrupole pairing interaction. The path is projected onto the (β, γ) potential energy surface. The dots in the figure indicate the HB local minima. Equipotential lines are drawn every 100 keV.

collective path for ^{68}Se obtained with the P+Q Hamiltonian including the quadrupole pairing interaction is very similar to that obtained in Ref. 75), in which its effect was ignored. As solutions of the ASCC equations, we obtain various quantities: the canonical collective coordinate q, the quadrupole deformations $\beta(q)$ and $\gamma(q)$, the monopole and quadruple pairing gaps $\Delta_0^{(\tau)}(q)$ and $\Delta_{2K}^{(\tau)}(q)$, the collective potential $V(q)$, the collective mass $M(s(q))$, the moving-frame QRPA frequency squared $\omega^2(q)$, and the three rotational moments of inertia $\mathcal{J}_i(q)$. These quantities are plotted in Fig. 2 as functions of $\gamma(q)$. It is seen that the quadrupole deformation $\beta(q)$ is almost constant along the collective path, while the triaxial deformation $\gamma(q)$ varies and

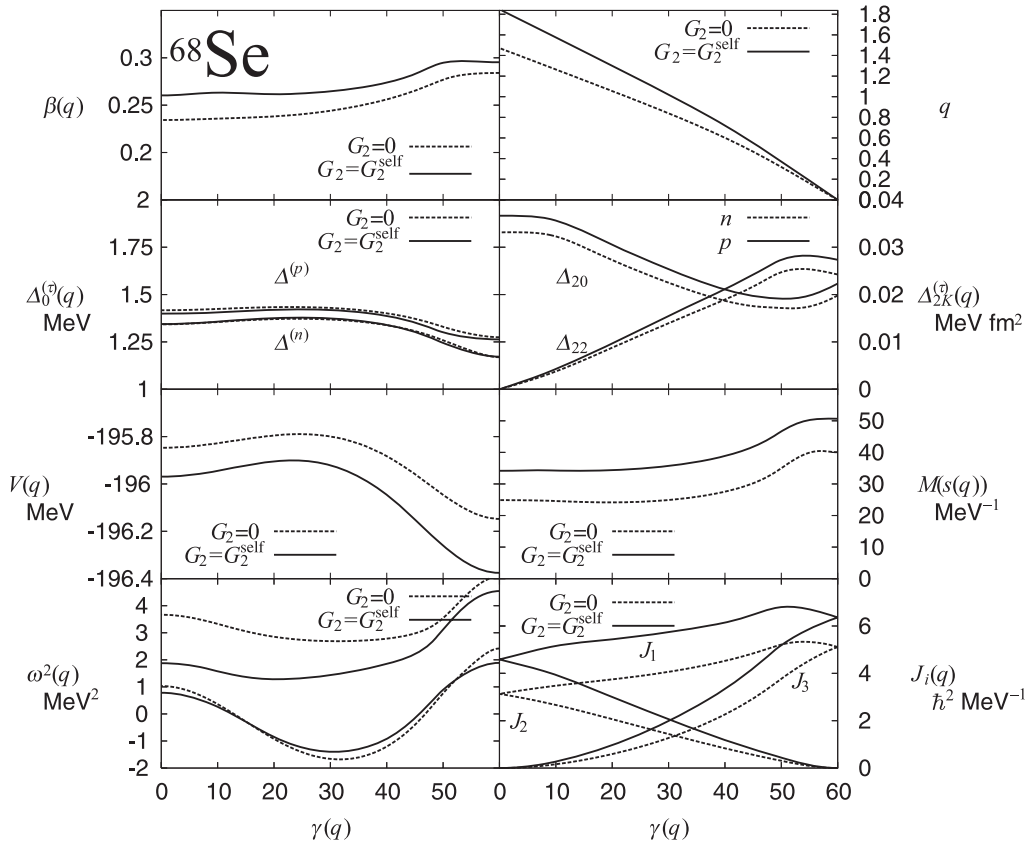

Fig. 2. Results of the calculation for ^{68}Se. The monopole pairing gap $\Delta_0^{(\tau)}(q)$, the quadrupole pairing gaps $\Delta_{20}^{(\tau)}(q)$ and $\Delta_{22}^{(\tau)}(q)$, the collective potential $V(q)$, the collective mass $M(s(q))$, the rotational moments of inertia $\mathcal{J}_i(q)$, the lowest two moving-frame QRPA frequencies squared $\omega^2(q)$, the axial quadrupole deformation $\beta(q)$, and the canonical collective coordinate q are plotted as functions of $\gamma(q)$. The results of the two calculations using the P+Q Hamiltonian with ($G_2 = G_2^{\rm self}$) and without ($G_2 = 0$) the quadrupole pairing interaction are compared.

changes from an oblate shape to a prolate shape. It is seen that the quadrupole pairing interaction slightly increases the values of $\beta(q)$ for all values of $\gamma(q)$.

The collective mass $M(s(q))$ plotted in Fig. 2 is defined as a function of the geometrical length, $ds = \sqrt{d\beta^2 + \beta^2 d\gamma^2}$, in the (β, γ) plane:

$$M(s(q)) = M(q)/\{(d\beta/dq)^2 + \beta^2(d\gamma/dq)^2\}. \tag{6·2}$$

As explained in §5.1, we can set $M(q) = B(q)^{-1} = 1\text{MeV}^{-1}$ here. We have found that the quadrupole pairing interaction increases the collective mass. This enhancement takes place almost independently of $\gamma(q)$, and it is mainly due to the decrease of $d\gamma/dq$ along the collective path.

Because the HB mean field becomes symmetric about the y'- and z'-axes in the oblate and prolate limits, respectively, the rotational moment of inertia about the y' (z')-axis vanishes, and the other two moments take the same values at the oblate (prolate) minimum. Their γ dependence is similar to that of the irrotational

moments of inertia. It is found the rotational moments of inertia increase by about $20-30\%$ through the effect of the quadrupole pairing interaction. This enhancement, as well as that of the inertial functions $M(s(q))$, is due to the time-odd pair field generated by the quadrupole pairing interaction.

6.4. *Collective path connecting the oblate and prolate minima in ^{72}Kr*

We have determined the collective path for ^{72}Kr starting from the oblate minimum. The collective path projected onto the (β, γ) plane is shown in Fig. 3, and various quantities defined along the collective path are plotted in Fig. 4 as functions of q. The collective paths calculated with and without the quadrupole pairing interaction are similar. Because the lowest mode of the moving-frame QRPA equations is β-vibrational around the oblate minimum, the path first goes along the axially symmetric line. Then, around $(\beta, \gamma) = (0.2, 60^\circ)$, the nature of the lowest mode changes to γ-vibrational, and thus the path deviates from the axially symmetric line. When the collective path reaches the $\gamma = 0^\circ$ line, the nature of the lowest mode again changes to β-vibrational. Approaching the prolate minimum, the nature of the lowest mode changes once more to γ-vibrational, and the collective path deviates from the $\gamma = 0^\circ$ line.

We note that the lowest two modes at the prolate local minimum are very close, and their ordering with respect to energy may be sensitive to the interactions used. We examined whether, for example, the lowest mode at the prolate local minimum becomes β-vibrational if the quadrupole pairing interaction is switched off, and in

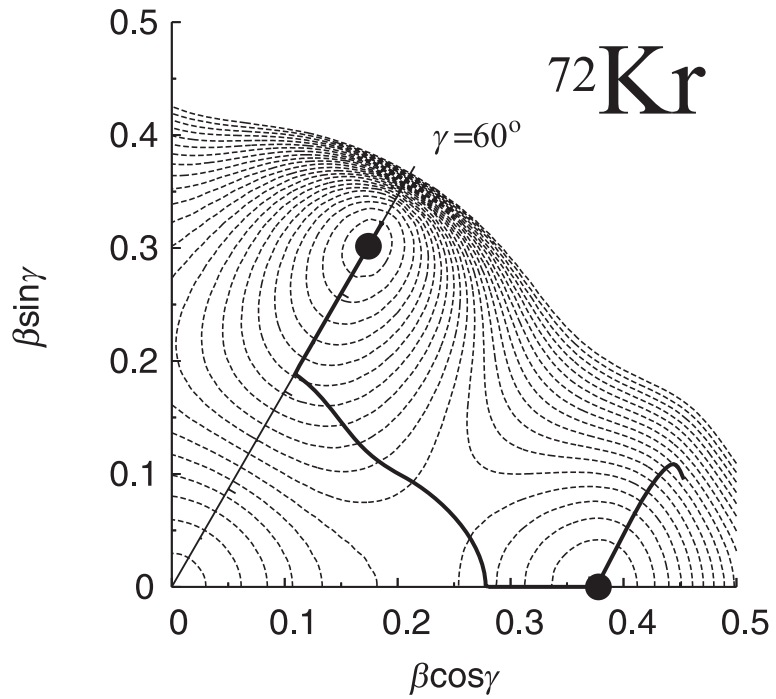

Fig. 3. The same as Fig. 1, but for ^{72}Kr.

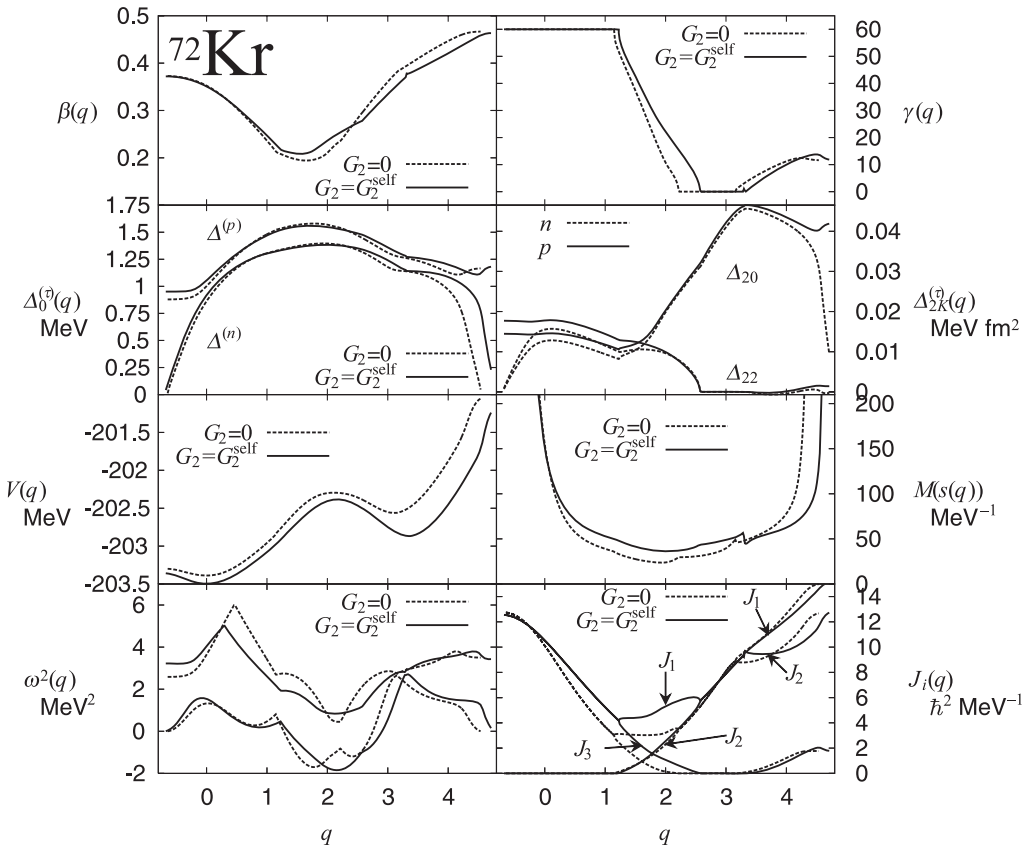

Fig. 4. Results of the calculations for ^{72}Kr. The notation here is the same as in Fig. 2, except that the quantities are plotted as functions of q along the collective path. The point $q = 0$ corresponds to the oblate minimum, while the prolate local minimum is located near $q = 3.3$ ($q = 3.1$) for the calculation using the P+Q Hamiltonian with (without) the quadrupole pairing interaction.

this case the axial symmetry breaking takes place at a larger value of β beyond the prolate local minimum. In such a situation, two collective coordinates may be needed to describe the collective dynamics more effectively. This is an interesting subject for future investigation. It should be emphasized that such a problem arises only locally in a small region in the (β, γ) plane, and the collective path is well-defined globally.

In the region of large β beyond the oblate minimum ($q < 0$) along the $\gamma = 60^\circ$ line, the lowest $K = 0$ mode exhibits a strong mixture of β-vibration (fluctuation of an axially symmetric shape) and neutron pairing vibration (fluctuation of pairing gaps), and the calculation to determine the collective path eventually stops when the neutron monopole pairing collapses.

We have found that the collective mass and the rotational moments of inertia increase also for ^{72}Kr, due to the time-odd pair field generated by the quadrupole pairing interaction. We note that the collective mass $M(s(q))$ diverges for large

deformations. This behavior, found also in previous works,[57),74),75)] is associated with the disappearance of the pairing gaps.

6.5. *Excitation spectra and quadrupole transitions in ^{68}Se*

The collective Schrödinger equation (5·2) was solved with the boundary conditions (5·14) and (5·17) for ^{68}Se to obtain energy spectra, quadrupole moments and transition probabilities. The results of the calculations are displayed in Fig. 5. The calculations yield the excited prolate rotational bands as well as the oblate ground state band. It is seen that the inter-band E2 transitions are weaker than the intra-band E2 transitions, indicating that the oblate-prolate shape coexistence picture is valid. The results of the calculation suggest the existence of an excited 0^+ state which has not yet been found in experiments. The spectroscopic quadrupole moments presented in Fig. 6 are also consistent with the oblate-prolate shape coexistence picture: The yrast states possess positive spectroscopic quadrupole moments, indicating oblate deformation, while the second lowest states for each angular momentum have negative values indicating prolate deformation. In Fig. 5, the excitation spectra calculated with and without the quadrupole pairing interaction are compared. We see that the quadrupole pairing plays an important role in decreas-

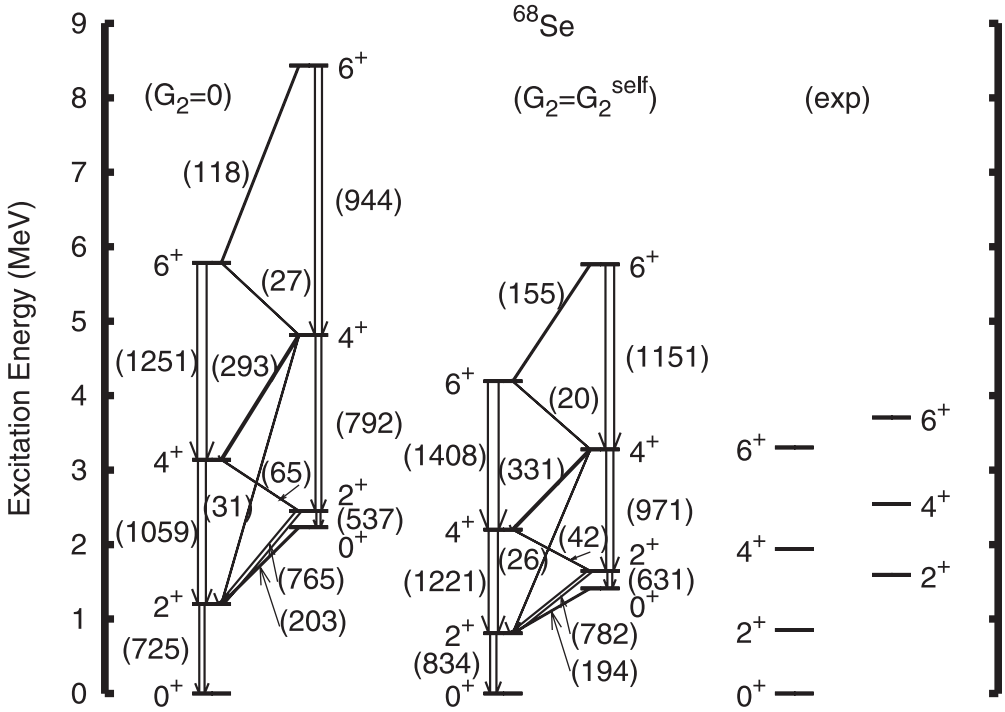

Fig. 5. Excitation spectra and B(E2) values of low-lying states in ^{68}Se calculated with the ASCC method. In the left (middle) panel, the quadrupole pairing is ignored (included) in the microscopic Hamiltonian. Experimental data[63)] are displayed in the right panel. The B(E2) values larger than 1 W.u. are indicated in the parentheses beside the arrows in units of e^2 fm^4.

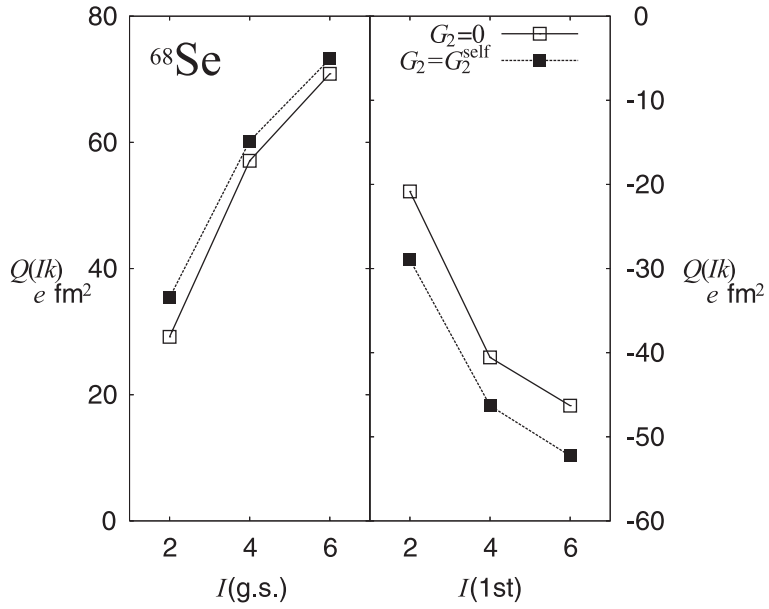

Fig. 6. Spectroscopic quadrupole moments of low-lying states in ^{68}Se. The left and right panels plot the spectroscopic quadrupole moments of the yrast states and of the second lowest states in each angular momentum, respectively. The units for the right panels are indicated beside the right vertical lines. The results of the calculations with (without) the quadrupole pairing interaction are indicated by the filled (open) squares.

ing the excitation energies. This is because the time-odd pair field generated by the quadrupole pairing enhances the collective mass and the rotational moments of inertia.

In Fig. 7, the vibrational wave functions are presented. It is seen that the behavior of the 0^+ states is significantly different from that of the $I \neq 0$ states: The vibrational wave functions of the lowest and the second lowest 0^+ states spread over the entire collective path, indicating that the oblate and prolate shapes are strongly mixed via the triaxial degree of freedom. In contrast to the 0^+ states, the $I \neq 0$ wave functions contain $K \neq 0$ components, which realize their maximum values in the oblate limit. We can see this trend more clearly by plotting the collective wave functions squared. This is done in Fig. 8. The vibrational wave function of the ground 0^+ state spreads over the entire region of γ, while that of the excited 0^+ state exhibits prominent peaks both in the oblate and prolate limits. By contrast, the vibrational wave functions of the $I \neq 0$ yrast states are localized around the oblate shape, while those of the second lowest states (for each angular momentum) are localized around the prolate shape. This localization becomes stronger with increasing angular momentum. In the yrast states, all the $K \neq 0$ components realize the maxima at the oblate shape, while the $K = 0$ component dominates at the prolate shape in the second lowest states.

In order to evaluate the oblate-prolate shape mixing in a more quantitative

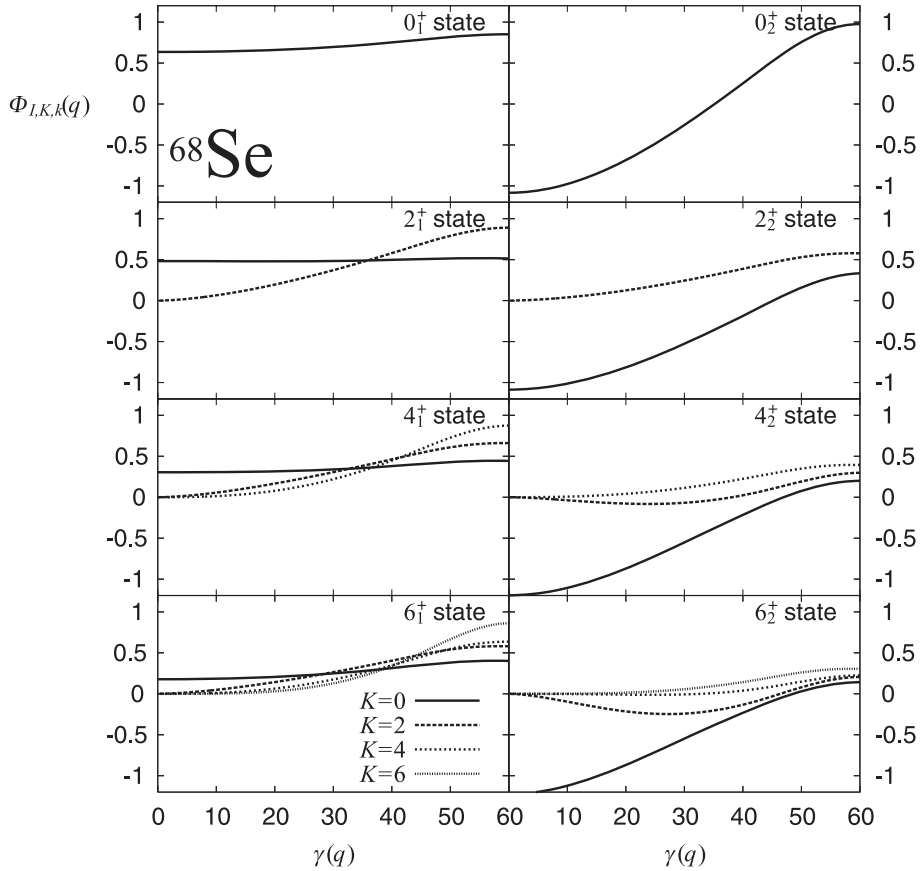

Fig. 7. Vibrational wave functions $\Phi_{IKk}(q)$ of the yrast states (*left*) and the second lowest states for each angular momentum (*right*) in ^{68}Se. In each panel, different K components of the vibrational wave functions are plotted as functions of $\gamma(q)$. The calculation was performed with the P+Q Hamiltonian including the quadrupole pairing interaction.

manner, we define the oblate and prolate probabilities as

$$P_{\rm ob}(I,k) = \int_{q_{\rm min}}^{q_0} dq \sum_{K=0}^{I} |\Phi_{IKk}(q)|^2, \quad P_{\rm pro}(I,k) = \int_{q_0}^{q_{\rm max}} dq \sum_{K=0}^{I} |\Phi_{IKk}(q)|^2, \quad (6{\cdot}3)$$

where we assume $q_{\rm min} \le q_{\rm ob} < q_0 < q_{\rm pro} \le q_{\rm max}$. The "boundary" between the oblate and the prolate regions is set to the top of the potential barrier between the two minima, or at $\gamma = 30^\circ$. Figure 9 displays these probabilities for ^{68}Se. The oblate and prolate states are strongly mixed in the 0^+ states. It is clearly seen that the shape mixing rapidly decreases as the angular momentum increases.

6.6. *Excitation spectra and quadrupole transitions in ^{72}Kr*

For ^{72}Kr, the collective Schrödinger equation is solved under the boundary conditions (5·18). The result of the calculation exhibits two coexisting rotational bands. [See the energy spectra and the B(E2) values displayed in Fig. 10.] The spectroscopic quadrupole moments presented in Fig. 11 indicate that the yrast band is

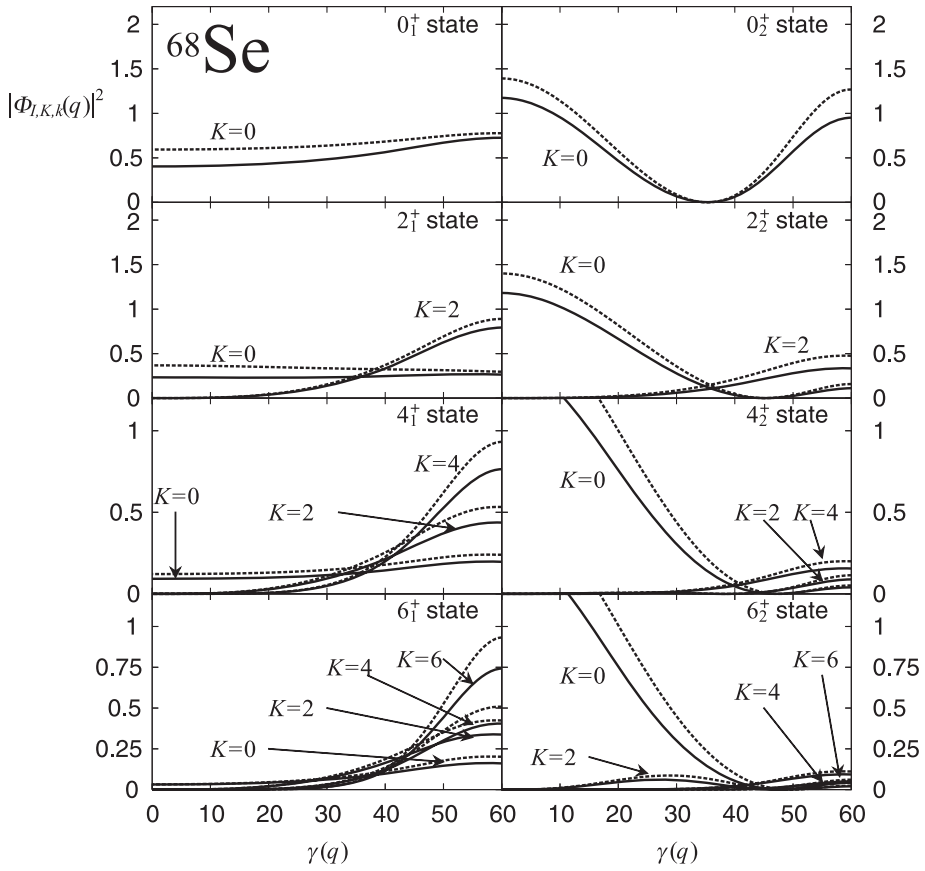

Fig. 8. Vibrational wave functions squared $|\Phi_{IKk}(q)|^2$ the yrast states (*left*), and the second lowest states at each angular momentum (*right*) for ^{68}Se. In each panel, different K components are plotted as functions of $\gamma(q)$. The solid (dashed) lines represent the results of calculations using the P+Q Hamiltonian with (without) the quadrupole pairing interaction. Note that the vibrational wave functions are normalized as in Eq. (5·9) with respect to the collective coordinate q, so that they are multiplied by the factor $d\gamma/dq$ when integrating with respect the triaxial deformation parameter γ. The $d\gamma/dq$ values calculated with the quadrupole pairing interaction are larger than those without it for all values of q.

oblate, while the excited band is prolate. For all states, including the 0^+ states, the inter-band B(E2) values are smaller by about one order of magnitude than the intra-band B(E2) values, and they rapidly decrease as the angular momentum increases. This indicates that the oblate-prolate shape mixing is rather weak in ^{72}Kr.

In Fig. 12, the vibrational wave functions are plotted. It is seen that the wave function of the 0_1^+ state is strongly localized in the oblate region, while that of the 0_2^+ state exhibits a major peak in the prolate region. In the yrast states with $I \neq 0$, localization about the oblate shape further develops for all K-components of the vibrational wave functions. The extent of this localization is larger for higher K. Contrastingly, the collective wave functions of the second lowest states in each angular momentum are essentially composed of the $K = 0$ component, which is

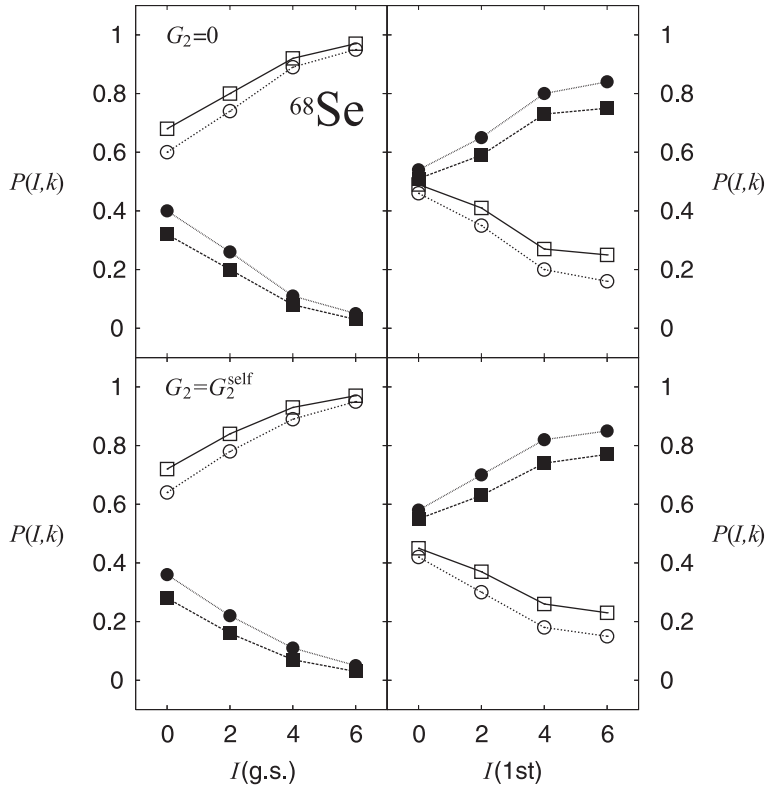

Fig. 9. The oblate and prolate probabilities evaluated for individual eigenstates of ^{68}Se. The upper (lower) panel plots the probabilities calculated using the P+Q Hamiltonian without (with) the quadrupole pairing interaction. The probabilities defined by setting the boundary at the barrier top ($\gamma = 30^\circ$) are indicated by squares (circles).

localized in the prolate region. Figure 13 plots the vibrational wave function squared. Rather weak oblate-prolate shape mixing is seen only for the excited 0^+ state, and other members of the rotational bands possess well-defined oblate or prolate forms. The oblate and prolate probabilities are presented in Fig. 14. It is seen that the shape mixing in the 0^+ states is much weaker than for ^{68}Se, and it almost vanishes at finite angular momentum.

§7. Concluding remarks

Shape coexistence/mixing phenomena in low-lying states of ^{68}Se and ^{72}Kr were investigated using the ASCC method. The excitation spectra, the spectroscopic quadrupole moments and the E2 transition properties of the low-lying states were evaluated for the first time using the ASCC method. We have derived the quantum collective Hamiltonian that describes the coupled collective motion of the large-amplitude vibration responsible for the oblate-prolate shape mixing and the three-dimensional rotation of the triaxial shape. The calculations yielded the excited prolate rotational band as well as the oblate ground-state band. The basic pattern of the

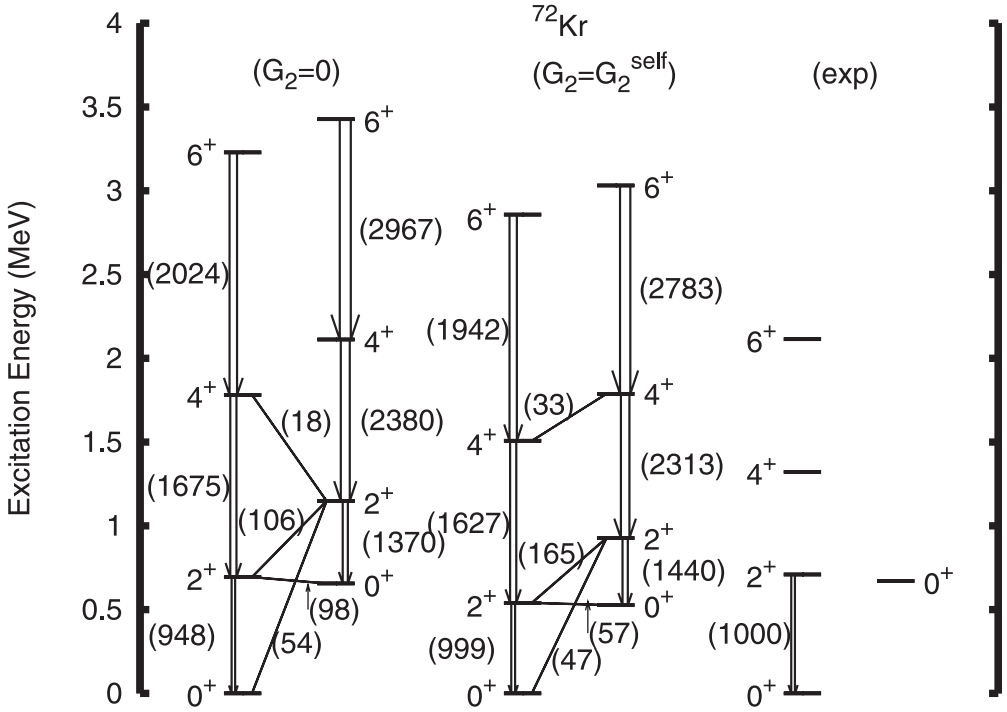

Fig. 10. The same as Fig. 5, but for ^{72}Kr. The experimental data are taken from Refs. 64)–66).

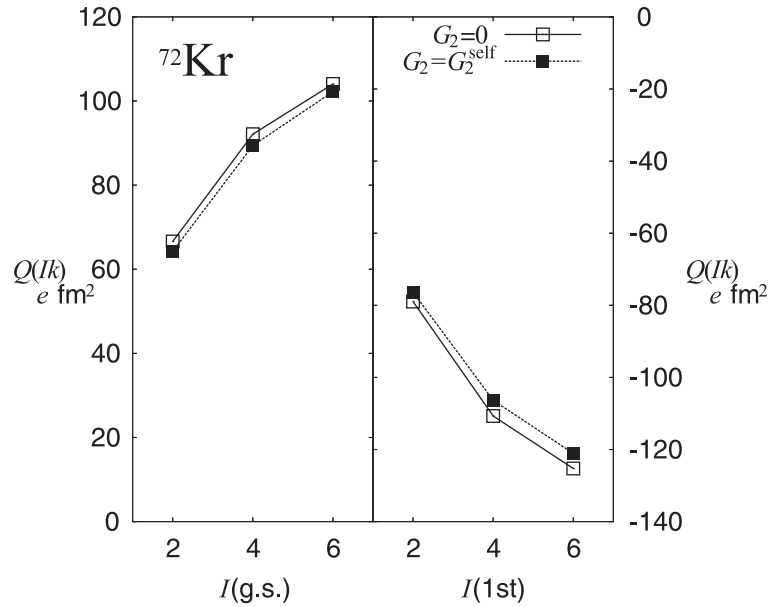

Fig. 11. The same as Fig. 6, but for ^{72}Kr. (See the caption of Fig. 6.)

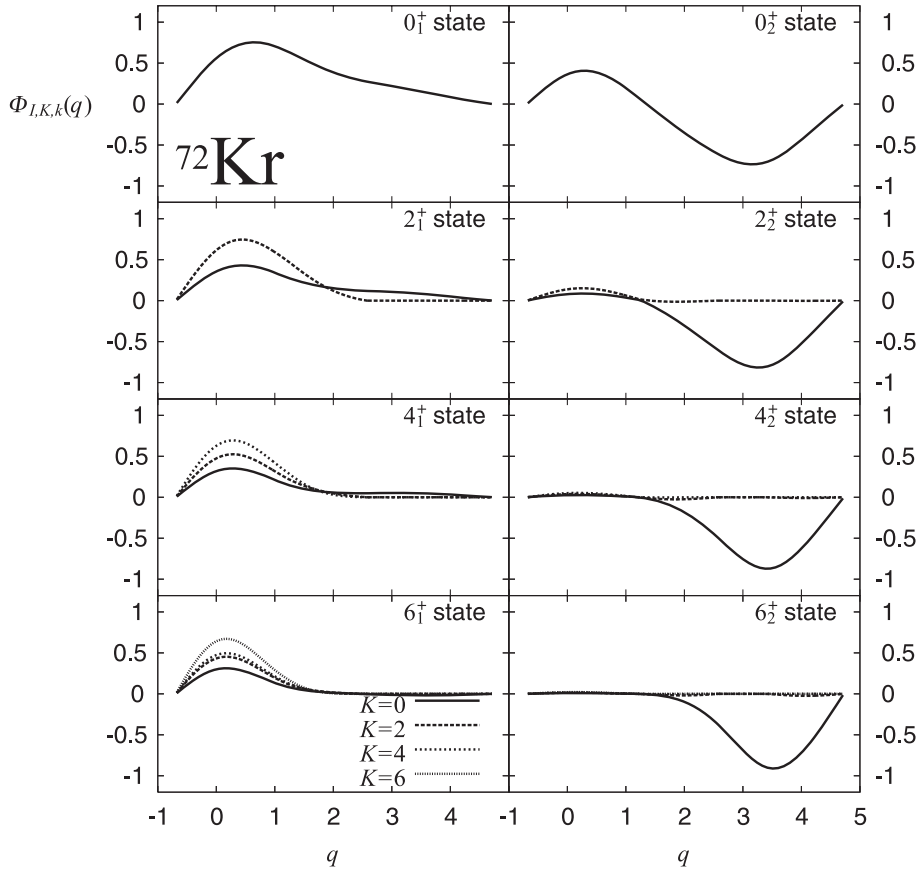

Fig. 12. Vibrational wave functions $\Phi_{IKk}(q)$ of low-lying states for ^{72}Kr plotted as functions of q. (See the caption of Fig. 7.)

shape coexistence/mixing phenomena has been qualitatively reproduced using the one-dimensional collective path in the two-dimensional (β, γ) plane. This collective path was self-consistently extracted from the many-dimensional TDHB manifold. Thus, the result of calculation indicates that the TDHB collective dynamics of the shape coexistence/mixing phenomena in these nuclei is essentially controlled by the single collective coordinate microscopically derived by means of the ASCC method.

We have also shown that the low-lying states can be described significantly more effectively by including the quadrupole pairing interaction. The reason for this is that the time-odd component of the mean field generated by the quadrupole pairing interaction enhances the collective mass of the vibrational motion and the moments of inertia of the rotational motion, and this lowers the energy of the collective excitation.

The present calculations clearly indicate that the oblate-prolate shape mixing decreases as the angular momentum increases. This implies that the rotational dynamics play the important role in realizing the localization of vibrational wave functions around the oblate and prolate minima in the situation that the barrier between these local minima is very low. We shall attempt a more detailed investigation

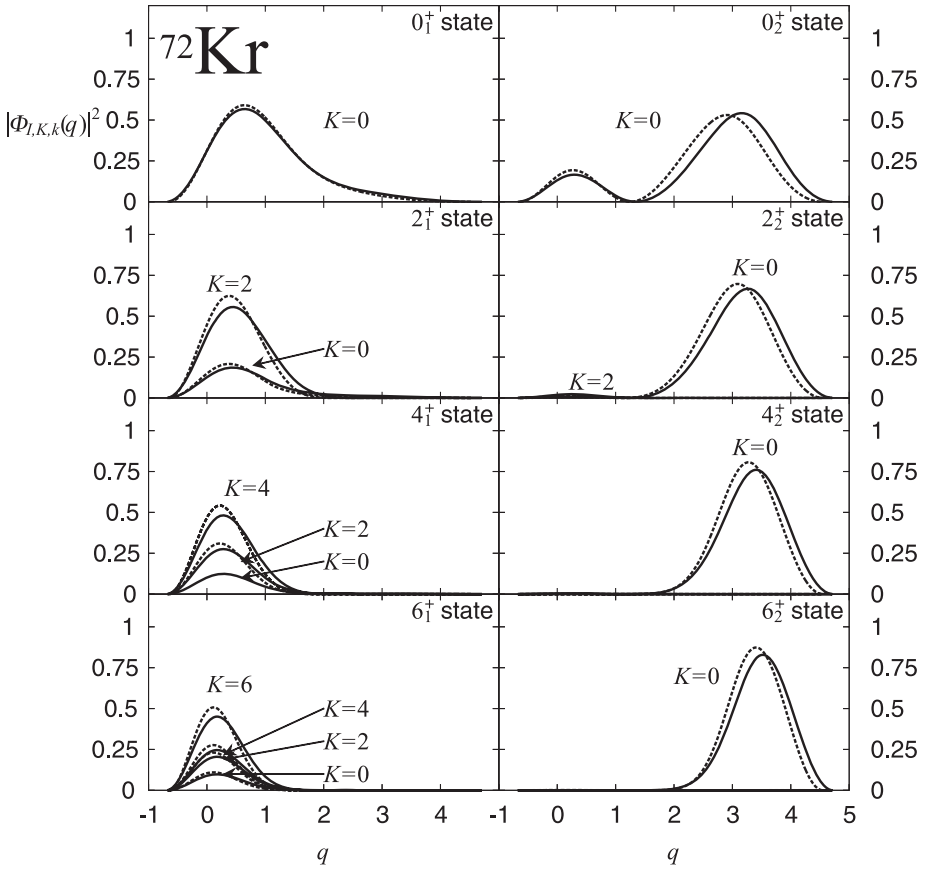

Fig. 13. Vibrational wave functions squared $|\Phi_{IKk}(q)|^2$ of low-lying states for ^{72}Kr plotted as functions of q. (See the caption of Fig. 8.)

of the dynamical reason why the rotational motion hinders the oblate-prolate shape mixing in a separate paper.

Acknowledgements

We thank Professors H. Aiba and S. Mizutori for useful discussions. This work is supported by Grants-in-Aid for Scientific Research (Nos. 18·2670, 16540249, 17540231, and 17540244) from the Japan Society for the Promotion of Science and the JSPS Core-to-Core Program "International Research Network for Exotic Femto Systems". We also thank the referee, whose comments were useful for improving the manuscript.

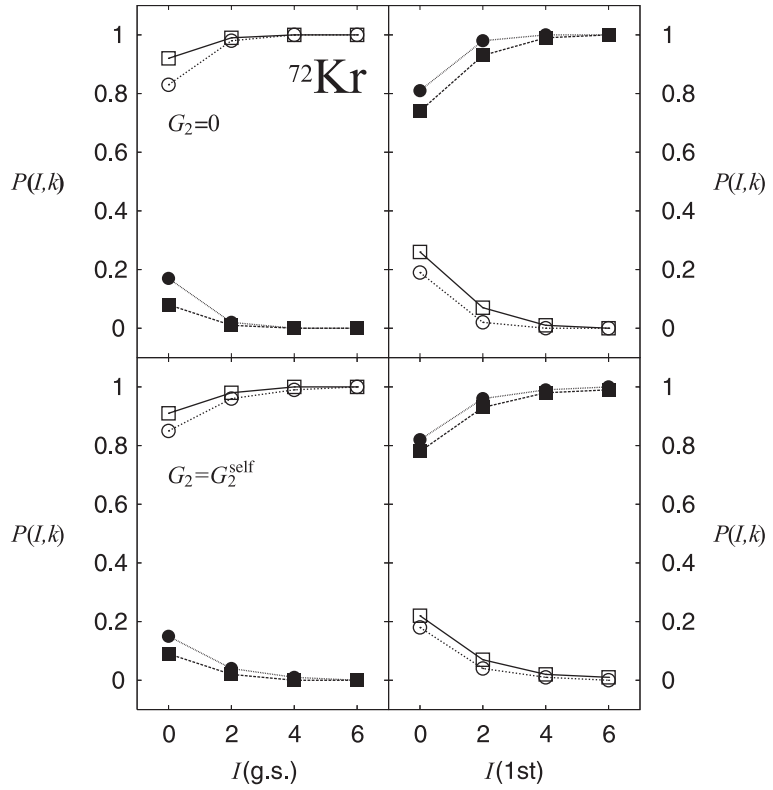

Fig. 14. The same as Fig. 9, but for ^{72}Kr.

Appendix A

Quasiparticle Representation of One-Body Operators

Because the moving mean field $|\phi(q)\rangle$ has positive signature, the conditions

$$U_{k\mu} = U_{\bar{k}\bar{\mu}}, \quad V_{k\bar{\mu}} = -V_{\bar{k}\mu}, \tag{A·1}$$

hold. The matrix elements of the pairing one-body operators $\hat{F}^{(\pm)}_{s=1,2,3,6,8,11}$ with $K = 0$ and 2 and $r = +1$ ($\hat{A}^{(\tau)(\pm)}$, $\hat{B}^{(\tau)(\pm)}_{20(+)}$, and $\hat{B}^{(\tau)(\pm)}_{22(+)}$) given in Eq. (4·24) are

$$\langle\phi(q)|\,\hat{F}^{(+)}_s\,|\phi(q)\rangle = 2{\sum_{\bar{k}l}}'(0|F^{(+)}_s|l\bar{k}){\sum_{\bar{\mu}}}' U_{\bar{k}\bar{\mu}}(q)V_{l\bar{\mu}}(q), \tag{A·2}$$

$$F^{(\pm)}_{A,s}(\mu\bar{\nu}) = {\sum_{k\bar{l}}}'(0|F^{(\pm)}_s|k\bar{l})(V_{k\bar{\nu}}(q)V_{\bar{l}\mu}(q) \pm U_{k\mu}(q)U_{\bar{l}\bar{\nu}}(q)), \tag{A·3}$$

$$F^{(\pm)}_{B,s}(\mu\nu) = {\sum_{k\bar{l}}}'(0|F^{(\pm)}_s|k\bar{l})(V_{\bar{l}\mu}(q)U_{k\nu}(q) \pm U_{k\mu}(q)V_{\bar{l}\nu}(q)). \tag{A·4}$$

The matrix elements of the particle-hole operators with $K = 0$ and 2 and $r = +1$ ($\hat{D}^{(+)}_{20}$ and $\hat{D}^{(+)}_{22}$) appearing in Eq. (4·24) are

$$\langle\phi(q)|\,\hat{F}^{(+)}_{s=13,15}\,|\phi(q)\rangle = 2{\sum_{kl}}'(k|F^{(+)}_{s=13,15}|l){\sum_{\mu}}'V_{k\bar{\mu}}(q)V_{l\bar{\mu}}(q), \tag{A·5}$$

$$F^{(+)}_{A,s=13,15}(\mu\bar{\nu}) = {\sum_{kl}}'(k|F^{(+)}_{s=13,15}|l)(U_{k\mu}(q)V_{l\bar{\nu}}(q) - U_{\bar{k}\bar{\nu}}(q)V_{\bar{l}\mu}(q)), \tag{A·6}$$

$$F^{(+)}_{B,s=13,15}(\mu\nu) = {\sum_{kl}}'(k|F^{(+)}_{s=13,15}|l)(U_{k\mu}(q)U_{l\nu}(q) - V_{\bar{k}\nu}(q)V_{\bar{l}\mu}(q)). \tag{A·7}$$

The matrix elements of the particle number operators given in Eq. (4·23) are

$$N^{(\tau)}(q) = \langle\phi(q)|\,\hat{N}^{(\tau)}\,|\phi(q)\rangle = 2{\sum_{k\in\tau}}'{\sum_{\bar{\mu}}}'V_{k\bar{\mu}}(q)^2, \tag{A·8}$$

$$N^{(\tau)}_A(\mu\bar{\nu}) = {\sum_{k\in\tau}}'(U_{k\mu}(q)V_{k\bar{\nu}}(q) - U_{\bar{k}\bar{\nu}}(q)V_{\bar{k}\mu}(q)), \tag{A·9}$$

$$N^{(\tau)}_B(\mu\nu) = {\sum_{k\in\tau}}'(U_{k\mu}(q)U_{k\nu}(q) - V_{\bar{k}\nu}(q)V_{\bar{k}\mu}(q)). \tag{A·10}$$

The constraint on the $\hat{Q}(q-\delta q)$ operator expressed by (4·21) in the moving-frame HB equation is written

$$\langle\phi(q)|\,\hat{Q}(q-\delta q)\,|\phi(q)\rangle = {\sum_{kl}}'Q_{kl}(q-\delta q){\sum_{\mu}}'V_{k\bar{\mu}}(q)V_{l\bar{\mu}}(q). \tag{A·11}$$

Appendix B
—— *Determination of the B-Part of* $\hat{Q}(q)$ ——

In this appendix, we show that the B-part of the operator ($\hat{Q}(q)$) can be determined through its A-part, ($\hat{Q}^A(q)$), which is obtained by solving the moving-frame QRPA equations. In terms of the quasiparticle operators, $a^\dagger_i$ and a_i, defined by the Bogoliubov transformation

$$\begin{pmatrix} c \\ c^\dagger \end{pmatrix} = \begin{pmatrix} U & V \\ V^* & U^* \end{pmatrix}\begin{pmatrix} a \\ a^\dagger \end{pmatrix}, \tag{B·1}$$

the Hermitian operator $\hat{Q}(q)$ is written

$$\begin{aligned}\hat{Q}(q) &= \sum_{ij} Q_{ij}(q)c^\dagger_i c_j \\ &= \sum_{ij}\left(Q^A_{ij}(q)a^\dagger_i a^\dagger_j + Q^{A*}_{ij}(q)a_j a_i + Q^B_{ij}(q)a^\dagger_i a_j\right),\end{aligned} \tag{B·2}$$

where

$$Q^A = U^\dagger Q V, \quad Q^B = U^\dagger Q U - V^\dagger Q V. \tag{B·3}$$

Thus, the matrices Q and Q^B can be written in terms of Q^A as

$$Q = (U^\dagger)^{-1} Q^A V^{-1}, \tag{B·4}$$

$$Q^B = Q^A V^{-1} U - V^\dagger (U^\dagger)^{-1} Q^A. \tag{B·5}$$

We cannot directly use these relations, however, to determine Q and Q^B, because the matrices Q and Q^B calculated using (B·4) and (B·5) are not Hermitian. For this reason, we have to construct Hermitian matrices Q and Q^B from Q^A. This is done by adding a symmetric matrix S to the solution of the moving-frame QRPA equation, which we here write Q_0^A, as

$$Q^A = Q_0^A + S. \tag{B·6}$$

For this matrix, Q is written

$$Q = (U^\dagger)^{-1}(Q_0^A + S)V^{-1} = Q_0 + (U^\dagger)^{-1} S V^{-1}, \tag{B·7}$$

$$Q^\dagger = (V^\dagger)^{-1}(Q_0^A + S)^\dagger U^{-1} = Q_0^\dagger + (V^\dagger)^{-1} S^\dagger U^{-1}. \tag{B·8}$$

From the Hermicity condition, $Q = Q^\dagger$, we obtain the following equation for S:

$$(V^\dagger)^{-1} S^\dagger U^{-1} - (U^\dagger)^{-1} S V^{-1} = Q_0 - Q_0^\dagger. \tag{B·9}$$

This determines the symmetric matrix S. Explicitly, the above equation is given by

$$\sum_{kl} \{(V^{-1})_{ki}(U^{-1})_{lj} - (U^{-1})_{ki}(V^{-1})_{lj}\} S_{kl} = (Q_0)_{ij} - (Q_0)_{ji}, \tag{B·10}$$

where we assume that all quantities are real. The number of unknown quantities and the number of equations are the same, $N(N+1)/2$, N being the dimension of the matrix. Therefore, it is possible to determine the matrix S by solving this equation.

In the case of the P+Q model, we start from the skew symmetric matrix Q_0^A,

$$(Q_0^A)_{\mu\bar{\nu}}(q) = \frac{1}{2} Q^A_{\mu\bar{\nu}}(q), \quad (Q_0^A)_{\bar{\nu}\mu}(q) = -\frac{1}{2} Q^A_{\mu\bar{\nu}}(q). \tag{B·11}$$

The symmetric matrix $S_{\mu\bar{\nu}} = S_{\bar{\nu}\mu}$ is determined by solving the equations,

$$\sum_{\mu\bar{\nu}}{}' \{(V^{-1})_{\bar{\nu}k}(U^{-1})_{\mu l} - (U^{-1})_{\mu k}(V^{-1})_{\bar{\nu}l}\} S_{\mu\bar{\nu}} = (Q_0)_{kl} - (Q_0)_{lk}, \tag{B·12}$$

$$\sum_{\mu\bar{\nu}}{}' \{(V^{-1})_{\mu\bar{k}}(U^{-1})_{\bar{\nu}\bar{l}} - (U^{-1})_{\bar{\nu}\bar{k}}(V^{-1})_{\mu\bar{l}}\} S_{\mu\bar{\nu}} = (Q_0)_{\bar{k}\bar{l}} - (Q_0)_{\bar{l}\bar{k}}, \tag{B·13}$$

where

$$(Q_0)_{kl}(q) = \sum_{\mu\bar{\nu}}{}' (U^{-1})_{\mu k}(Q_0^A)_{\mu\bar{\nu}}(q)(V^{-1})_{\bar{\nu}l}, \tag{B·14}$$

$$(Q_0)_{\bar{k}\bar{l}}(q) = \sum_{\mu\bar{\nu}}{}' (U^{-1})_{\bar{\nu}\bar{k}}(Q_0^A)_{\bar{\nu}\mu}(q)(V^{-1})_{\mu\bar{l}}. \tag{B·15}$$

As the relation $(Q_0^A)_{\mu\bar{\nu}} = (Q_0^A)_{\nu\bar{\mu}}$ holds, the matrix S satisfies the relation $S_{\mu\bar{\nu}} = -S_{\nu\bar{\mu}}$, and thus, Eqs. (B·12) and (B·13) are written

$$\sum_{\mu\bar{\nu}}{}' \{-(V^{-1})_{\bar{\nu}k}(U^{-1})_{\mu l} - (U^{-1})_{\nu k}(V^{-1})_{\bar{\mu}l}\} S_{\mu\bar{\nu}} = (Q_0)_{kl} - (Q_0)_{lk}. \tag{B·16}$$

Using the transformed matrix $Q^{A'}(q)$,

$$Q^{A'}_{\mu\bar{\nu}}(q) = (Q_0^A)_{\mu\bar{\nu}}(q) + S_{\mu\bar{\nu}}, \tag{B·17}$$

the Hermite matrices $Q(q)$ and $Q^B(q)$ are obtained as follows:

$$Q_{kl}(q) = \sum_{\mu\bar{\nu}}{}' (U^{-1})_{\mu k} Q^{A'}_{\mu\bar{\nu}}(q) (V^{-1})_{\bar{\nu}l}, \tag{B·18}$$

$$Q_{\bar{k}\bar{l}}(q) = \sum_{\bar{\mu}\nu}{}' (U^{-1})_{\bar{\mu}\bar{k}} Q^{A'}_{\bar{\mu}\nu}(q) (V^{-1})_{\nu\bar{l}}, \tag{B·19}$$

$$Q^B_{\mu\nu}(q) = \sum_{kl}{}' U_{k\mu} Q_{kl}(q) U_{l\nu} - V_{\bar{k}\mu} Q_{\bar{k}\bar{l}}(q) V_{\nu\bar{l}}, \tag{B·20}$$

$$Q^B_{\bar{\mu}\bar{\nu}}(q) = \sum_{\bar{k}\bar{l}}{}' U_{\bar{\mu}\bar{k}} Q_{\bar{k}\bar{l}}(q) U_{\bar{l}\bar{\nu}} - V_{k\bar{\mu}} Q_{kl}(q) V_{l\bar{\nu}}. \tag{B·21}$$

Appendix C

—— *Calculation of the Rotational Moments of Inertia* ——

For the separable interactions (3·7), the Thouless-Valatin equations (2·26) determining the three rotational moments of inertia, $\mathcal{J}_i(q)$, about the principal axes in a non-equilibrium state $|\phi(q)\rangle$ can be written in the form

$$\delta \langle\phi(q)| [\hat{h}_M(q), \hat{\Psi}_i(q)] + i \sum_s f^{(+)}_{\Psi_i,s}(q) \hat{F}^{(+)}_s - \sum_s f^{(-)}_{\Psi_i,s}(q) \hat{F}^{(-)}_s - \frac{1}{i} \mathcal{J}_i^{-1}(q) \hat{I}_i |\phi(q)\rangle = 0, \tag{C·1}$$

where

$$f^{(+)}_{\Psi_i,s}(q) = i\kappa_s \langle\phi(q)| [\hat{F}^{(+)}_s, \hat{\Psi}_i(q)] |\phi(q)\rangle , \tag{C·2}$$

$$f^{(-)}_{\Psi_i,s}(q) = -\kappa_s \langle\phi(q)| [\hat{F}^{(-)}_s, \hat{\Psi}_i(q)] |\phi(q)\rangle . \tag{C·3}$$

The quasiparticle representation of the angular momentum operators is expressed as

$$\hat{I}_x = \sum_{\mu\nu}{}' I_{A,x}(\mu\bar{\nu})(\boldsymbol{A}^\dagger_{\mu\bar{\nu}} + \boldsymbol{A}_{\mu\bar{\nu}}) + \sum_{\mu\nu}{}' I_{B,x}(\mu\nu)(\boldsymbol{B}_{\mu\nu} - \boldsymbol{B}_{\bar{\mu}\bar{\nu}}), \tag{C·4}$$

$$i\hat{I}_y = \sum_{\mu\nu}{}' I_{A,y}(\mu\nu)(\boldsymbol{A}^\dagger_{\mu\nu} - \boldsymbol{A}_{\mu\nu}) + I_{A,y}(\bar{\mu}\bar{\nu})(\boldsymbol{A}^\dagger_{\bar{\mu}\bar{\nu}} - \boldsymbol{A}_{\bar{\mu}\bar{\nu}}) + \sum_{\mu\nu}{}' I_{B,y}(\mu\bar{\nu})(\boldsymbol{B}_{\mu\bar{\nu}} - \boldsymbol{B}_{\bar{\mu}\nu}), \tag{C·5}$$

$$\hat{I}_z = \sum_{\mu\nu}{}' I_{A,z}(\mu\nu)(\boldsymbol{A}^\dagger_{\mu\nu} + \boldsymbol{A}_{\mu\nu}) + I_{A,z}(\bar{\mu}\bar{\nu})(\boldsymbol{A}^\dagger_{\bar{\mu}\bar{\nu}} + \boldsymbol{A}_{\bar{\mu}\bar{\nu}}) + \sum_{\mu\nu}{}' I_{B,z}(\mu\bar{\nu})(\boldsymbol{B}_{\mu\bar{\nu}} + \boldsymbol{B}_{\bar{\mu}\nu}), \tag{C·6}$$

where the matrix elements of $I_{A,x}, I_{A,y}$ and $I_{A,z}$ are given by

$$I_{A,x}(\mu\bar{\nu}) = \sum_{kl}{}' (k|I_x|l)(U_{k\mu}(q)V_{l\bar{\nu}}(q) + U_{\bar{k}\bar{\nu}}(q)V_{\bar{l}\mu}(q)), \tag{C·7}$$

$$I_{A,y}(\mu\nu) = I_{A,y}(\bar{\mu}\bar{\nu}) = \sum_{kl}{}' (k|I_y|l)U_{k\mu}(q)V_{\bar{l}\nu}(q), \tag{C·8}$$

$$I_{A,z}(\mu\nu) = -I_{A,z}(\bar{\mu}\bar{\nu}) = -\sum_{k}{}' m_k U_{k\mu}(q)V_{\bar{k}\nu}(q). \tag{C·9}$$

The residual interactions with $(r = +1, K = 1)$, $(r = -1, K = 1)$ and $(r = -1,\ K = 2)$ contribute to rotations about the x, y and z-axis, respectively. The quasiparticle representation of the one-body operators having these quantum numbers is given by

$$\hat{F}^{(\pm)}_s = \sum_{\mu\bar{\nu}}{}' F^{(\pm)}_{A,s}(\mu\bar{\nu})(\boldsymbol{A}^\dagger_{\mu\bar{\nu}} \pm \boldsymbol{A}_{\mu\bar{\nu}}) + \sum_{\mu\nu}{}' F^{(\pm)}_{B,s}(\mu\nu)(\boldsymbol{B}_{\mu\nu} - \boldsymbol{B}_{\bar{\mu}\bar{\nu}}), \quad (r = +1, K = 1) \tag{C·10}$$

$$\hat{F}^{(\pm)}_s = \sum_{\mu\nu}{}' F^{(\pm)}_{A,s}(\mu\nu)(\boldsymbol{A}^\dagger_{\mu\nu} \pm \boldsymbol{A}_{\mu\nu} + \boldsymbol{A}^\dagger_{\bar{\mu}\bar{\nu}} \pm \boldsymbol{A}_{\bar{\mu}\bar{\nu}}) + \sum_{\mu\nu}{}' F^{(\pm)}_{B,s}(\mu\bar{\nu})(\boldsymbol{B}_{\mu\bar{\nu}} - \boldsymbol{B}_{\bar{\mu}\nu}), \quad (r = -1, K = 1) \tag{C·11}$$

$$\hat{F}^{(\pm)}_s = \sum_{\mu\nu}{}' F^{(\pm)}_{A,s}(\mu\nu)\{\boldsymbol{A}^\dagger_{\mu\nu} \pm \boldsymbol{A}_{\mu\nu} - (\boldsymbol{A}^\dagger_{\bar{\mu}\bar{\nu}} \pm \boldsymbol{A}_{\bar{\mu}\bar{\nu}})\} + \sum_{\mu\nu}{}' F^{(\pm)}_{B,s}(\mu\bar{\nu})(\boldsymbol{B}_{\mu\bar{\nu}} + \boldsymbol{B}_{\bar{\mu}\nu}). \quad (r = -1, K = 2) \tag{C·12}$$

The matrix elements of the quadrupole pairing operators are

$$F^{(\pm)}_{A,s=4,9}(\mu\bar{\nu}) = 2\sum_{kl\in\tau}{}' (0|B^{(\tau)(\pm)}_{21(-)}|k\bar{l})(V_{\bar{l}\mu}(q)V_{k\bar{\nu}}(q) \pm U_{k\mu}(q)U_{\bar{l}\bar{\nu}}(q)), \tag{C·13}$$

$$F^{(\pm)}_{A,s=5,10}(\mu\nu) = \sum_{kl\in\tau}{}' (0|B^{(\tau)(\pm)}_{21(+)}|kl)(V_{l\bar{\mu}}(q)V_{k\bar{\nu}}(q) \pm U_{\bar{k}\bar{\mu}}(q)V_{\bar{l}\bar{\nu}}(q)), \tag{C·14}$$

$$F^{(\pm)}_{A,s=7,12}(\mu\nu) = \sum_{kl\in\tau}{}' (0|B^{(\tau)(\pm)}_{22(-)}|kl)(-V_{\bar{l}\mu}(q)V_{\bar{k}\nu}(q) \pm U_{k\mu}(q)U_{l\nu}(q)), \tag{C·15}$$

$$F^{(\pm)}_{A,s=5,10}(\mu\nu) = F^{(\pm)}_{A,s=5,10}(\bar{\mu}\bar{\nu}), \quad F^{(\pm)}_{A,s=7,12}(\mu\nu) = -F^{(\pm)}_{A,a=7,12}(\bar{\mu}\bar{\nu}). \tag{C·16}$$

Note that the quadrupole operators $\hat{D}^{(\pm)}_{21}$ and $\hat{D}^{(-)}_{22}$ do not contribute to the moments of inertia.

The three Thouless-Valatin equations, appearing in (C·1), for a non-equilibrium state can be solved independently. The angle operators $\hat{\Psi}_x(q), \hat{\Psi}_y(q)$ and $\hat{\Psi}_z(q)$ can be written as

$$\hat{\Psi}_x(q) = i{\sum_{\mu\bar{\nu}}}' \Psi_{A,x}(\mu\bar{\nu})(\boldsymbol{A}^\dagger_{\mu\bar{\nu}} - \boldsymbol{A}_{\mu\bar{\nu}}) + (\boldsymbol{B} - \text{part}), \tag{C·17a}$$

$$\hat{\Psi}_y(q) = {\sum_{\mu\nu}}' \Psi_{A,y}(\mu\nu)(\boldsymbol{A}^\dagger_{\mu\nu} + \boldsymbol{A}_{\mu\nu}) + \Psi_{A,y}(\bar{\mu}\bar{\nu})(\boldsymbol{A}^\dagger_{\bar{\mu}\bar{\nu}} + \boldsymbol{A}_{\bar{\mu}\bar{\nu}}) + (\boldsymbol{B}-\text{part}), \tag{C·17b}$$

$$\hat{\Psi}_z(q) = i{\sum_{\mu\nu}}' \Psi_{A,z}(\mu\nu)(\boldsymbol{A}^\dagger_{\mu\nu} - \boldsymbol{A}_{\mu\nu}) + \Psi_{A,z}(\bar{\mu}\bar{\nu})(\boldsymbol{A}^\dagger_{\bar{\mu}\bar{\nu}} - \boldsymbol{A}_{\bar{\mu}\bar{\nu}}) + (\boldsymbol{B}-\text{part}). \tag{C·17c}$$

These matrix elements are easily obtained from Eq. (C·1) as

$$\Psi_{A,x}(\mu\bar{\nu}) = \frac{-1}{E_\mu + E_{\bar{\nu}}} \left(\sum_s f^{(+)}_{\Psi_x,s}(q) F^{(+)}_{A,s}(\mu\bar{\nu}) + \mathcal{J}_x^{-1}(q) I_{A,x}(\mu\bar{\nu}) \right), \tag{C·18a}$$

$$\Psi_{A,y}(\mu\nu) = \frac{1}{E_\mu + E_\nu} \left(\sum_s f^{(-)}_{\Psi_y,s}(q) F^{(-)}_{A,s}(\mu\nu) - \mathcal{J}_y^{-1}(q) I_{A,y}(\mu\nu) \right), \tag{C·18b}$$

$$\Psi_{A,y}(\bar{\mu}\bar{\nu}) = \frac{1}{E_{\bar{\mu}} + E_{\bar{\nu}}} \left(\sum_s f^{(-)}_{\Psi_y,s}(q) F^{(-)}_{A,s}(\bar{\mu}\bar{\nu}) - \mathcal{J}_y^{-1}(q) I_{A,y}(\bar{\mu}\bar{\nu}) \right), \tag{C·18c}$$

$$\Psi_{A,z}(\mu\nu) = \frac{1}{E_\mu + E_\nu} \left(-\sum_s f^{(+)}_{\Psi_z,s}(q) F^{(+)}_{A,s}(\mu\nu) - \mathcal{J}_z^{-1}(q) I_{A,z}(\mu\nu) \right), \tag{C·18d}$$

$$\Psi_{A,z}(\bar{\mu}\bar{\nu}) = \frac{1}{E_{\bar{\mu}} + E_{\bar{\nu}}} \left(-\sum_s f^{(+)}_{\Psi_z,s}(q) F^{(+)}_{A,s}(\bar{\mu}\bar{\nu}) - \mathcal{J}_z^{-1}(q) I_{A,z}(\bar{\mu}\bar{\nu}) \right). \tag{C·18e}$$

It is easy to confirm that $f^{(-)}_{\Psi_x,s}(q) = 0, f^{(+)}_{\Psi_y,s}(q) = 0$ and $f^{(-)}_{\Psi_z,s}(q) = 0$. Substituting (C·18) into the quantities $f^{(+)}_{\Psi_x,s}(q), f^{(-)}_{\Psi_y,s}(q)$ and $f^{(+)}_{\Psi_z,s}(q)$ and the canonical variable condition (2·26), we obtain

$$\begin{aligned} f^{(+)}_{\Psi_x,s}(q) &= i\kappa_s \langle\phi(q)| [\hat{F}^{(+)}_s, \hat{\Psi}_x(q)] |\phi(q)\rangle \\ &= 2\kappa_s \sum_{s'} (F^{(+)}_{A,s}, F^{(+)}_{A,s'})_{E+} f^{(+)}_{\Psi_x,s'}(q) + 2\kappa_s (F^{(+)}_{A,s}, I_{A,x})_{E+} \mathcal{J}_x^{-1}(q), \end{aligned} \tag{C·19a}$$

$$\begin{aligned} f^{(-)}_{\Psi_y,s}(q) =& -\kappa_s \langle\phi(q)| [\hat{F}^{(-)}_s, \hat{\Psi}_y] |\phi(q)\rangle \\ =& 2\kappa_s \sum_{s'} (F^{(-)}_{A,s}, \overline{F^{(-)}_{A,s'}})_{E-} f^{(-)}_{\Psi_y,s'}(q) - 2\kappa_s (F^{(-)}_{A,s}, \overline{I_{A,y}})_{E-} \mathcal{J}_y^{-1}(q), \end{aligned} \tag{C·19b}$$

$$\begin{aligned} f^{(+)}_{\Psi_z,s}(q) =& i\kappa_s \langle\phi(q)| [\hat{F}^{(+)}_s, \hat{\Psi}_z(q)] |\phi(q)\rangle \\ =& 2\kappa_s \sum_{s'} (F^{(+)}_{A,s}, \overline{I_{A,z}})_{E-} f^{(+)}_{\Psi_z,s'}(q) + 2\kappa_s (F^{(+)}_{A,s}, \overline{I_{A,z}})_{E-} \mathcal{J}_z^{-1}(q), \end{aligned} \tag{C·19c}$$

$$\langle\phi(q)| [\hat{\Psi}_x(q), \hat{I}_x] |\phi(q)\rangle / i = -2{\sum_{\mu\bar{\nu}}}' \Psi_{A,x}(\mu,\bar{\nu}) I_{A,x}(\mu\bar{\nu})$$

$$= -2\sum_{s}(F^{(+)}_{A,s}, I_{A,x})_{E+} f^{(+)}_{\Psi_x,s}(q) - 2(I_{A,x}, I_{A,x})_{E+}\mathcal{J}_x^{-1}(q)$$
$$= 1, \tag{C·20a}$$
$$\langle\phi(q)|\,[\hat{\Psi}_y(q), i\hat{I}_y]\,|\phi(q)\rangle = 2{\sum_{\mu\nu}}' \Psi_{A,y}(\mu\nu)\overline{I_{A,y}}(\mu\nu) + 2{\sum_{\bar{\mu}\bar{\nu}}}' \Psi_{A,y}(\bar{\mu}\bar{\nu})\overline{I_{A,y}}(\bar{\mu}\bar{\nu})$$
$$= 2\sum_{s}(F^{(-)}_{A,s}, \overline{I_{A,y}})_{E-} f^{(-)}_{\Psi_y,s}(q) - 2(I_{A,y}, \overline{I_{A,y}})_{E-}\mathcal{J}_y^{-1}(q)$$
$$= -1, \tag{C·20b}$$
$$\langle\phi(q)|\,[\hat{\Psi}_z(q), \hat{I}_z]\,|\phi(q)\rangle\,/i = -2{\sum_{\mu\nu}}' \Psi_{A,z}(\mu\nu)\overline{I_{A,z}}(\mu\nu) - 2{\sum_{\bar{\mu}\bar{\nu}}}' \Psi_{A,z}(\bar{\mu}\bar{\nu})\overline{I_{A,z}}(\bar{\mu}\bar{\nu})$$
$$= 2\sum_{s}(F^{(+)}_{A,s}, \overline{I_{A,z}})_{E-} f^{(+)}_{\Psi_z,s'}(q) + 2(I_{A,z}, \overline{I_{A,z}})_{E-}\mathcal{J}_z^{-1}(q)$$
$$= 1, \tag{C·20c}$$

where

$$(X, Y)_{E+} = {\sum_{\mu\bar{\nu}}}' \frac{X(\mu\bar{\nu})Y(\mu\bar{\nu})}{E_\mu + E_{\bar{\nu}}}, \tag{C·21}$$
$$\overline{X}(\mu\nu) = X(\mu\nu) - X(\nu\mu), \tag{C·22}$$
$$(X, Y)_{E-} = {\sum_{\mu\nu}}' \frac{X(\mu\nu)Y(\mu\nu)}{E_\mu + E_\nu} + {\sum_{\bar{\mu}\bar{\nu}}}' \frac{X(\bar{\mu}\bar{\nu})Y(\bar{\mu}\bar{\nu})}{E_{\bar{\mu}} + E_{\bar{\nu}}}. \tag{C·23}$$

Equations (C·19) and (C·20) are linear equations with respect to $f^{(+)}_{\Psi_i,s}(q)$ and $\mathcal{J}_i^{-1}(q)$, and they can be rewritten as follows:

$$\sum_{s'}\begin{pmatrix} 2\kappa_s(F^{(+)}_{A,s}, F^{(+)}_{A,s'})_{E+} - \delta_{ss'} & 2\kappa_{s'}(F^{(+)}_{A,s}, I_{A,x})_{E+} \\ 2(F^{(+)}_{A,s}, I_{A,x})_{E+} & 2(I_{A,x}, I_{A,x})_{E+}, \end{pmatrix}\begin{pmatrix} f^{(+)}_{\Psi_x,s'}(q) \\ \mathcal{J}_x^{-1}(q) \end{pmatrix} = \begin{pmatrix} 0 \\ 1 \end{pmatrix}, \tag{C·24a}$$

$$\sum_{s'}\begin{pmatrix} 2\kappa_s(F^{(-)}_{A,s}, \overline{F^{(-)}_{A,s'}})_{E-} - \delta_{ss'} & -2\kappa_s(F^{(-)}_{A,s}, \overline{I_{A,y}})_{E-} \\ -2(F^{(-)}_{A,s}, \overline{I_{A,y}})_{E-} & 2(I_{A,y}, \overline{I_{A,y}})_{E-} \end{pmatrix}\begin{pmatrix} f^{(-)}_{\Psi_y,s}(q) \\ \mathcal{J}_y^{-1} \end{pmatrix} = \begin{pmatrix} 0 \\ 1 \end{pmatrix}, \tag{C·24b}$$

$$\sum_{s'}\begin{pmatrix} 2\kappa_s(F^{(+)}_{A,s}, \overline{F^{(+)}_{A,s}})_{E-} - \delta_{ss'} & 2\kappa_s(F^{(+)}_{A,s}, \overline{I_{A,z}})_{E-} \\ 2(F^{(+)}_{A,s'}, \overline{I_{A,z}})_{E-} & 2(I_{A,z}, \overline{I_{A,z}})_{E-} \end{pmatrix}\begin{pmatrix} f^{(+)}_{\Psi_z,s'}(q) \\ \mathcal{J}_z^{-1}(q) \end{pmatrix} = \begin{pmatrix} 0 \\ 1 \end{pmatrix}. \tag{C·24c}$$

References

1) P. Ring and P. Schuck, *The Nuclear Many-Body Problem* (Springer-Verlag, 1980).
2) J.-P. Blaizot and G. Ripka, *Quantum Theory of Finite Systems* (The MIT press, 1986).
3) A. Abe and T. Suzuki (ed.), Prog. Theor. Phys. Suppl. Nos. 74 & 75 (1983), 1.
4) D. M. Brink and R. A. Broglia, *Nuclear Superfluidity, Pairing in Finite Systems* (Cambridge University Press, 2005).

5) A. Bohr and B. R. Mottelson, *Nuclear Structure*, Vol. II (W. A. Benjamin Inc., 1975; World Scientific, 1998).
6) D. J. Rowe and R. Bassermann, Can. J. Phys. **54** (1976), 1941.
7) D. M. Brink, M. J. Giannoni and M. Vénéroni, Nucl. Phys. A **258** (1976), 237.
8) F. Villars, Nucl. Phys. A **285** (1977), 269.
9) T. Marumori, Prog. Theor. Phys. **57** (1977), 112.
10) M. Baranger and M. Veńéroni, Ann. of Phys. **114** (1978), 123.
11) K. Goeke and P.-G. Reinhard, Ann. of Phys. **112** (1978), 328.
12) T. Marumori, T. Maskawa, F. Sakata and A. Kuriyama, Prog. Theor. Phys. **64** (1980), 1294.
13) M. J. Giannoni and P. Quentin, Phys. Rev. C **21** (1980), 2060; Phys. Rev. C **21** (1980), 2076.
14) J. Dobaczewski and J. Skalski, Nucl. Phys. A **369** (1981), 123.
15) K. Goeke, P.-G. Reinhard and D. J. Rowe, Nucl. Phys. A **359** (1981), 408.
16) A. K. Mukherjee and M. K. Pal, Phys. Lett. B **100** (1981), 457; Nucl. Phys. A **373** (1982), 289.
17) D. J. Rowe, Nucl. Phys. A **391** (1982), 307.
18) C. Fiolhais and R. M. Dreizler, Nucl. Phys. A **393** (1983), 205.
19) P.-G. Reinhard, F. Grümmer and K. Goeke, Z. Phys. A **317** (1984), 339.
20) A. Kuriyama and M. Yamamura, Prog. Theor. Phys. **70** (1983), 1675; Prog. Theor. Phys. **71** (1984), 122.
21) M. Yamamura, A. Kuriyama and S. Iida, Prog. Theor. Phys. **71** (1984), 109.
22) M. Matsuo and K. Matsuyanagi, Prog. Theor. Phys. **74** (1985), 288.
23) M. Matsuo, Prog. Theor. Phys. **76** (1986), 372.
24) Y. R. Shimizu and K. Takada, Prog. Theor. Phys. **77** (1987), 1192.
25) M. Yamamura and A. Kuriyama, Prog. Theor. Phys. Suppl. No. 93 (1987), 1.
26) A. Bulgac, A. Klein, N. R. Walet and G. Do Dang, Phys. Rev. C **40** (1989), 945.
27) N. R. Walet, G. Do Dang and A. Klein, Phys. Rev. C **43** (1991), 2254.
28) A. Klein, N. R. Walet and G. Do Dang, Ann. of Phys. **208** (1991), 90.
29) K. Kaneko, Phys. Rev. C **49** (1994), 3014.
30) T. Nakatsukasa and N. R. Walet, Phys. Rev. C **57** (1998), 1192.
31) T. Nakatsukasa and N. R. Walet, Phys. Rev. C **58** (1998), 3397.
32) T. Nakatsukasa, N. R. Walet and G. Do Dang, Phys. Rev. C **61** (1999), 014302.
33) J. Libert, M. Girod and J.-P. Delaroche, Phys. Rev. C **60** (1999), 054301.
34) E. Kh. Yuldashbaeva, J. Libert, P. Quentin and M. Girod, Phys. Lett. B **461** (1999), 1.
35) L. Próchniak, P. Quentin, D. Samsoen and J. Libert, Nucl. Phys. A **730** (2004), 59.
36) D. Almehed and N. R. Walet, Phys. Rev. C **69** (2004), 024302.
37) D. Almehed and N. R. Walet, Phys. Lett. B **604** (2004), 163.
38) D. Almehed and N. R. Walet, J. of Phys. G **31** (2005), S1523.
39) D. Almehed and N. R. Walet, nucl-th/0509079.
40) A. Klein and E. R. Marshalek, Rev. Mod. Phys **63** (1991), 375.
41) G. Do Dang, A. Klein and N. R. Walet, Phys. Rep. **335** (2000), 93.
42) A. Kuriyama, K. Matsuyanagi, F. Sakata, K. Takada and M. Yamamura (Ed.), Prog. Theor. Phys. Suppl. No. 141 (2001), 1.
43) M. Matsuo, Prog. Theor. Phys. **72** (1984), 666.
44) M. Matsuo and K. Matsuyanagi, Prog. Theor. Phys. **74** (1985), 1227; Prog. Theor. Phys. **76** (1986), 93; Prog. Theor. Phys. **78** (1987), 591.
45) M. Matsuo, Y. R. Shimizu and K. Matsuyanagi, *Proceedings of The Niels Bohr Centennial Conf. on Nuclear Structure*, ed. R. Broglia, G. Hagemann and B. Herskind (North-Holland, 1985), p. 161.
46) M. Matsuo, in *New Trends in Nuclear Collective Dynamics*, ed. Y. Abe, H. Horiuchi and K. Matsuyanagi (Springer-Verlag, 1992), p. 219.
47) K. Takada, K. Yamada and H. Tsukuma, Nucl. Phys. A **496** (1989), 224.
48) K. Yamada, K. Takada and H. Tsukuma, Nucl. Phys. A **496** (1989), 239.
49) K. Yamada and K. Takada, Nucl. Phys. A **503** (1989), 53.
50) K. Yamada, Prog. Theor. Phys. **85** (1991), 805; Prog. Theor. Phys. **89** (1993), 995.
51) H. Aiba, Prog. Theor. Phys. **84** (1990), 908.
52) J. Terasaki, T. Marumori and F. Sakata, Prog. Theor. Phys. **85** (1991), 1235.

53) J. Terasaki, Prog. Theor. Phys. **88** (1992), 529; Prog. Theor. Phys. **92** (1994), 535.
54) Y. R. Shimizu and K. Matsuyanagi, Prog. Theor. Phys. Suppl. No. 141 (2001), 285.
55) M. Matsuo, T. Nakatsukasa and K. Matsuyanagi, Prog. Theor. Phys. **103** (2000), 959.
56) N. Hinohara, T. Nakatsukasa, M. Matsuo and K. Matsuyanagi, Prog. Theor. Phys. **117** (2007), 451.
57) N. Hinohara, T. Nakatsukasa, M. Matsuo and K. Matsuyanagi, Prog. Theor. Phys. **115** (2006), 567.
58) K. Matsuyanagi, Prog. Theor. Phys. **67** (1982), 1441; *Proceedings of the Nuclear Physics Workshop*, Trieste, 5-30 Oct. 1981, ed. C. H. Dasso, R. A. Broglia and A. Winther (North-Holland, 1982), p. 29.
59) Y. Mizobuchi, Prog. Theor. Phys. **65** (1981), 1450.
60) T. Suzuki and Y. Mizobuchi, Prog. Theor. Phys. **79** (1988), 480.
61) T. Fukui, M. Matsuo and K. Matsuyanagi, Prog. Theor. Phys. **85** (1991), 281.
62) J. L. Wood, K. Heyde, W. Nazarewicz, M. Huyse and P. van Duppen, Phys. Rep. **215** (1992), 101.
63) S. M. Fischer et al., Phys. Rev. Lett. **84** (2000), 4064.
64) S. M. Fischer et al., Phys. Rev. C **67** (2003), 064318.
65) E. Bouchez et al., Phys. Rev. Lett. **90** (2003), 082502.
66) A. Gade et al., Phys. Rev. Lett. **95** (2005), 022502 [Errata; **96** (2006), 189901].
67) M. Yamagami, K. Matsuyanagi and M. Matsuo, Nucl. Phys. A **693** (2001), 579.
68) K. Kaneko, M. Hasegawa and T. Mizusaki, Phys. Rev. C **70** (2004), 051301.
69) K. Langanke, D. J. Dean and W. Nazarewicz, Nucl. Phys. A **728** (2003), 109.
70) M. Bender, P. Bonche and P.-H. Heenen, Phys. Rev. C **74** (2006), 024312.
71) A. Petrovici, K. W. Schmid and A. Faessler, Nucl. Phys. A **710** (2002), 246.
72) A. Petrovici, K. W. Schmid and A. Faessler, Nucl. Phys. A **605** (1996), 290.
73) A. Petrovici, K. W. Schmid and A. Faessler, Nucl. Phys. A **665** (2000), 333.
74) M. Kobayasi, T. Nakatsukasa, M. Matsuo and K. Matsuyanagi, Prog. Theor. Phys. **110** (2003), 65.
75) M. Kobayasi, T. Nakatsukasa, M. Matsuo and K. Matsuyanagi, Prog. Theor. Phys. **112** (2004), 363; Prog. Theor. Phys. **113** (2005), 129.
76) D. R. Bes and R. A. Sorensen, *Advances in Nuclear Physics* vol. 2 (Prenum Press, 1969), p. 129.
77) M. Baranger and K. Kumar, Nucl. Phys. **62** (1965), 113; Nucl. Phys. A **110** (1968), 529; Nucl. Phys. A **122** (1968), 241; Nucl. Phys. A **122** (1968), 273.
78) M. Baranger and K. Kumar, Nucl. Phys. A **110** (1968), 490.
79) K. Kumar and M. Baranger, Nucl. Phys. A **92** (1967), 608.
80) D. J. Thouless and G. J. Valatin, Nucl. Phys. **31** (1962), 211.
81) N. Hinohara, T. Nakatsuaksa, M. Matsuo and K. Matsuyanagi, to be published in *Proceedings of International Symposium on Physics of Unstable Nuclei (ISPUN07)*, Hoi An, Vietnam, 3-7 July 2007 (World Scientific); arXiv:0709.3897.
82) H. Sakamoto and T. Kishimoto, Phys. Lett. B **245** (1990), 321.